DETECTION OF A LOW LEVEL SIGNAL IN NOISE BY TEGULOMETRIC METHODS

Kiefer Ault Tobin

NAVAL POSTGRADUATE SCHOOL
Monterey, California

THESIS

DETECTION OF A LOW LEVEL SIGNAL IN NOISE
BY TEGULOMETRIC METHODS

by

Kiefer Ault Tobin

December, 1976

Thesis Advisor: George Marmont

UNCLASSIFIED

SECURITY CLASSIFICATION OF THIS PAGE (When Data Entered)

REPORT DOCUMENTATION PAGE		READ INSTRUCTIONS BEFORE COMPLETING FORM
1. REPORT NUMBER	2. GOVT ACCESSION NO.	3. RECIPIENT'S CATALOG NUMBER
4. TITLE (and Subtitle) Detection of a Low Level Signal in Noise by Tegulometric Methods		5. TYPE OF REPORT & PERIOD COVERED Master's Thesis December, 1976 6. PERFORMING ORG. REPORT NUMBER
7. AUTHOR(s) Kiefer Ault Tobin		8. CONTRACT OR GRANT NUMBER(s)
9. PERFORMING ORGANIZATION NAME AND ADDRESS Naval Postgraduate School Monterey, Ca. 93940		10. PROGRAM ELEMENT, PROJECT, TASK AREA & WORK UNIT NUMBERS
11. CONTROLLING OFFICE NAME AND ADDRESS Naval Postgraduate School Monterey, Ca. 93940		12. REPORT DATE December, 1976 13. NUMBER OF PAGES 89
14. MONITORING AGENCY NAME & ADDRESS(if different from Controlling Office) Naval Postgraduate School Monterey, Ca. 93940		15. SECURITY CLASS. (of this report) UNCLASSIFIED 15a. DECLASSIFICATION/DOWNGRADING SCHEDULE

16. DISTRIBUTION STATEMENT (of this Report)

Approved for public release; Distribution unlimited

17. DISTRIBUTION STATEMENT (of the abstract entered in Block 20, if different from Report)

18. SUPPLEMENTARY NOTES

19. KEY WORDS (Continue on reverse side if necessary and identify by block number)

Tegulometric
Signal processing
Signal to noise
Acoustic data analysis
Ideal digital filter
Histogram

20. ABSTRACT (Continue on reverse side if necessary and identify by block number)

A novel and sensitive method is described for the analysis and detection of weak signals generated by many sources and highly contaminated by noise. This process yields a spectral display whose elements are related to the probability of occurrence of a frequency rather than to the power spectral density of conventional schemes. Thus, a weak signal and stronger signals may show equally if they appear over the same percentage of the analysis period.

DD FORM 1 JAN 73 1473 EDITION OF 1 NOV 65 IS OBSOLETE
S/N 0102-014-6601 |
(Page 1)

UNCLASSIFIED

SECURITY CLASSIFICATION OF THIS PAGE (When Data Entered)

This process, called tegulometric analysis, is tested and improved in sensitivity for detection of very weak signals hidden in gaussian noise. The investigation shows that this method can be optimized to produce low level signal detections based upon short observational periods. The frequency resolution capability of the method is shown to be marked.

DETECTION OF A LOW LEVEL SIGNAL IN NOISE BY TEGULOMETRIC METHODS

by

Kiefer Ault Tobin
Lieutenant Commander
B.S., Oregon State University, 1960

Submitted in partial fulfillment of the
requirements for the degree of

MASTER OF SCIENCE IN ENGINEERING ACOUSTICS

from the

NAVAL POSTGRADUATE SCHOOL

December 1976

ABSTRACT

A novel and sensitive method is described for the analysis and detection of weak signals generated by many sources and highly contaminated by noise. This process yields a spectral display whose elements are related to the probability of occurrence of a frequency rather than to the power spectral density of conventional schemes. Thus, a weak signal and stronger signals may show equally if they appear over the same percentage of the analysis period.

This process, called tegulometric analysis, is tested and improved in sensitivity for detection of very weak signals hidden in gaussian noise. The investigation shows that this method can be optimized to produce low level signal detections based upon short observational periods. The frequency resolution capability of the method is shown to be marked.

TABLE OF CONTENTS

LIST OF FIGURES

ACKNOWLEDGEMENT

Acknowledgement is given to Professor George Marmont of the U. S. Postgraduate School who initiated the method of tegulometric analysis and continues to provide the insight and impetus to its continuing development. His great patience, insight and expertise in many areas provided the foundations for this work.

The Naval Electronics Systems Command (NAVELEX 304) provided support during the earlier phases of the investigation.

The unfailing moral support and understanding of my wife and family contributed immeasurably to the completion of this work.

I. INTRODUCTION

A. BACKGROUND

Tegulometric signal processing techniques originated in the electroencephalographic (EEG) work by Dr. George Marmont in 1973 at the U. S. Naval Postgraduate School. In analyzing the narrow band filtered EEG data, he observed that the waveforms in each band appeared as a series of sinusoids within an envelope lasting about 0.1 second. These spindle-like structures were the result of the algebraic summation of electrical changes taking place within many activity centers in the brain. This waxing and waning structure was defined as a tegule which is shown on Fig 1. The envelope of a typical train of tegules exhibits periods of high amplitudes followed by significant periods of low amplitude. Further analysis revealed that the tegules in one band were seldom coincident with tegules in other bands, showing that results were not due to the impulse response of the filter. Initial investigation into tegulometric analysis was accomplished by S. E. Dollar [Ref. 3] and W. E. Stockslager [Ref. 6] with Dr. Marmont.

Separate observations of narrow band ocean acoustic data in phonograms also revealed a similar tegular nature. The periods in which the envelope was low were not as long as in the EEG data but much longer than would be observed from a beating phenomenon. In the case of acoustic data, however, the tegules resulted from the complex superposition of signals from many sources within the filter band over many

paths and possessing random amplitude and phase. Because of this, the method of tegulometric analysis appeared to have potential application in analyzing acoustic data. Such an investigation was conducted by T. J. Colyer [Ref. 2] who demonstrated that weak acoustic signals in random noise could be detected and identified by this method. Since electromagnetic signals suffer many of the same interference problems to which acoustic signals are subjected, it is expected that tegulometric analysis should have equal value to radar, communications, ESM, and other low signal-to-noise applications.

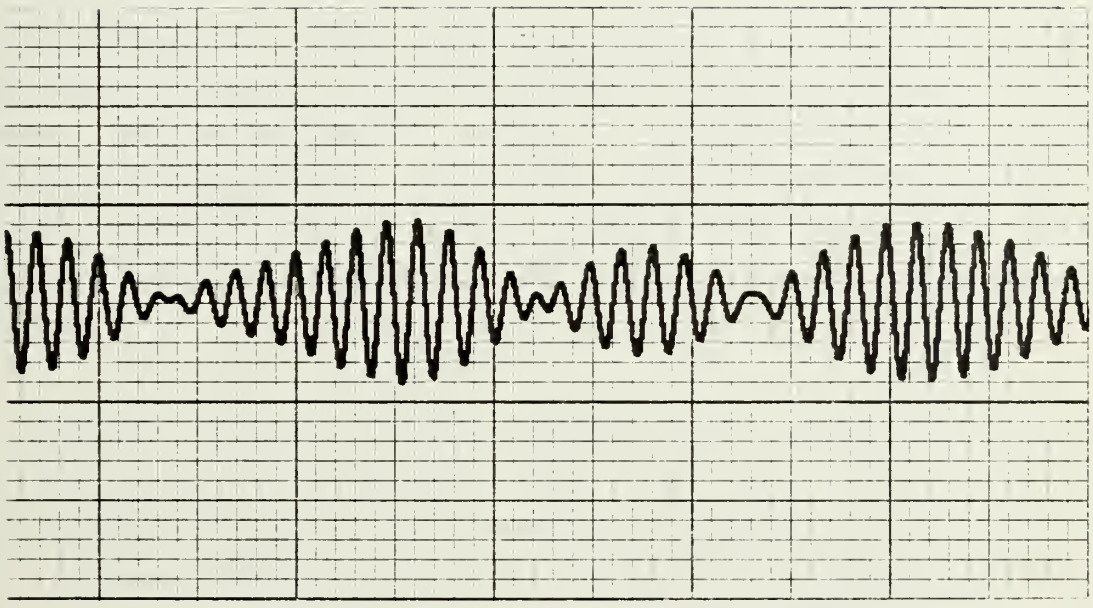

Figure 1 - TYPICAL TEGULES

B. OBJECTIVES

Previous research had tested many of the aspects of tegulometric analysis and applied this scheme to specific problems. The results of these investigations demonstrated that this technique was not only very useful, but also could be a novel method for the detection and identification of very weak signals buried in non-stationary noise.

The purpose of this investigation was to more thoroughly test each processing step to assure that the results of this process were accurate and valid. A second objective, after successful completion of these tests, was established to improve the sensitivity of the analysis so that even weaker signals could be detected when hidden by many other sources of noise.

Because a number of the concepts are novel, this thesis first provides a description of both the basis and the processing scheme of tegulometric analysis. Next, tests of the key routines are discussed including equipment used and general test philosophy. The subsequent section deals with the methods used to improve analysis sensitivity and includes techniques which varied in success from marginal to excellent. Finally, the most promising sensitivity improvement methods are combined in a series of tests and the results are presented.

C. ADVANTAGES OF TEGULOMETRIC ANALYSIS

Previous work pointed out a number of advantages in this

method. The first is that tegulometric analysis of acoustic signals is more sensitive and possess a higher degree of frequency resolution than the discrete fourier transform (DFT). Part of this effect is believed due to not fully exploiting phase information by the DFT in that only the magnitudes of the resultant complex frequency elements are displayed. Alternately, tegulometric analysis depends heavily on the magnitude and phase of the signal and noise.

Because this technique analyzes relatively short time sample windows, the results are not as affected by non-stationary data resulting from multipath transmission or fluctuations of the transmission medium. This modulation by the non-linear transmission medium will tend to spread the signal in frequency and phase, causing conventional fine-grained frequency techniques to be degraded. Further research in this area remains to be done.

II. DESCRIPTION OF TEGULOMETRIC ANALYSIS

A. BASIS OF THE METHOD

Observation of the time domain representation of wide band noise reveals its complex nature. In the narrow band, this noise exibits the waxing and waning behavior noted in the introduction and defined as tegules.

Trace A of Fig 2 is the time representation of wide band noise. A narrow band filtered representation of the same noise over the same time period is shown on trace C which clearly demonstrates the tegular nature of filtered noise. The random frequency elements within the filter add to produce periods where the noise not only can be a minimum, but also can result in phase reversal. During these intervals of low amplitude, a weak signal can capture the noise to appear within these minima. Trace B is derived from the data of trace C except that a weak signal has been inserted within the filter. Note that the signal, although very weak in magnitude, momentarily captures the surrounding noise and appears. If the presence of this signal during the noise cancellation periods could be observed and counted, a potentially very sensitive detection method would result. It is precisely this phenomenon that tegulometric analysis exploits.

As a measure of the probability of occurrence of the weak signal, it is possible to measure the time between negative to positive zero crossings of the filtered data and

to convert this time to an equivalent frequency. A spectral block is created in the memory in which each successive word corresponds to an equivalent frequency number. For each negative to positive zero crossing, the equivalent frequency is computed and its respective memory location is incremented by one count. This spectral block is therefore a histogram whose amplitude, frequency dependent, is a measure of the probability density function (pdf) of the frequencies of the noise plus any signals. Since even a weak signal will be present while the noise varies according to its pdf, it is expected that this more persistent signal will appear as an increase in the histogram.

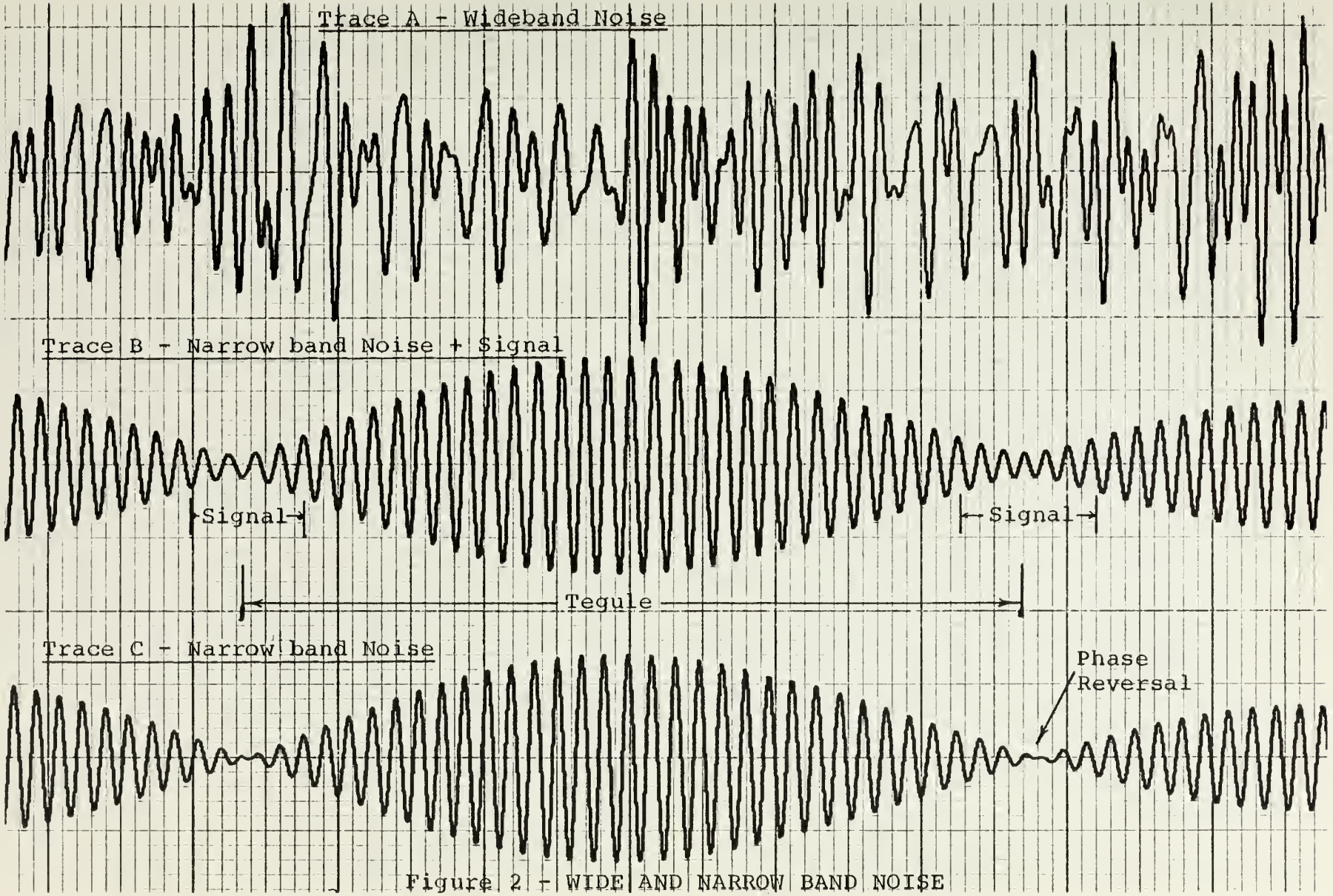

Figure 2 - WIDE AND NARROW BAND NOISE

B. PROCESSING SCHEME

1. Definitions

All work for this thesis was performed on a 16 bit digital computer for which each data storage location was defined as a "word" containing an integer number. Because the computer installation had the capability of addressing by 8 bit bytes, addresses for words are even numbered (increment by 2). A complex number is represented by two successive words, the first being the real, integer part and the second the imaginary, integer part. The complex pair is referred to as a complex element or element.

The data is handled in much of the programming as blocks of information. The advantage of this method is to allow the block of data to be treated as a single entity in performing operations on data. This allows data manipulation by a single instruction without resorting to loops. An example might be a single call to ADDBLOCK B0,B1 which adds block, B0, to block, B1. In order to perform this, each block has a table (Block Identification Block) which contains the number of block words, the type of block (real or complex), the absolute address of the first word of the block, and the block exponent. The block exponent is the binary exponent which applies to all words in that block. This technique allows processing in integer arithmetic to reduce core storage requirements while allowing a greater dynamic range of the data. This scheme is required by the hardware fast fourier transform (FFT) peripheral used in this investigation. Block length is described in the number of "K" words, where $1K = 1024 = 2^{10}$

words according to common usage.

The ratio of signal power to noise power requires definition since its magnitude depends upon the bandwidth of the noise . For this report, bandwidth will be defined to be 1 Hz so that for noise of bandwidth W_b , and root mean square (rms) voltage of σ , and signal of amplitude A, the signal to noise ratio will be:

$$S/N = \frac{A^2/2}{\sigma^2/W_b}$$

In discussing the programs and results to follow, it is important to define frequency. If each sample block (time domain) consisted of N samples which were sampled at a rate of R, then the time, T represented by this block of data was:

$$T = N/R$$

Further, if the sampled waveform was limited to W Hz, the discrete transform will have N/2 complex frequency elements whose frequency separation was Δf, then:

$$\Delta f = 1/T$$

Since all data in this investigation was handled in 4K blocks (4096 samples), N was constant at 4096 words. Further, to prevent aliasing in the direct Fourier transform (DFT), the Nyquist sampling rate was always adhered to so that:

$$W = R/2$$

Therefore, once a sample rate was selected, all other parameters were uniquely defined. These relations were adhered to in the recording of all analog signals with the result that actual time ceased to be meaningful in digital form. The relation between "real time" and "digital time",

then, was simply the sample rate.

Because of this, it became convenient to define total sample time, T, as 1 second so that the frequency separation in the DFT was 1 Hz. The bandwidth was 2048 Hz and the "sample rate" was 4096 samples per second. To relate to the "real world", all that was needed was the application of the ratio of R/4096 to the various parameters.

The convention described above is adhered to in this thesis for ease of discussion. Where time in seconds or frequency in Hertz is noted, the quantities will refer to "digital" time.

2. Memory Map

The data memory map for HISCAN, the main program which performs the tegulometric analysis, is shown in Fig 3. Block designations are shown as B0, B1, etc. The numbers in parentheses indicate the length of the blocks in "K" words. A brief description of the various blocks is as follows:

a. Block B0 - used for input and temporary storage of sampled data.

b. Block B8 - initially contains sampled data, loaded from B0. It subsequently contains the spectral block associated with sampled data.

c. Blocks B4 and B9 - used in the transfer of sampled data from B0 to B8. B9 is also used to filter (zero) the upper half of the spectral block.

d. Blocks B10, B2, B15, B11 - ideal filter blocks. B10 contains a copy of a complex-complex form of the spectral block in B8. Blocks B2, B15, and B11 are used to zero the appropriate frequency elements of the filter.

e. Block B5 - Overlays B10 so that after the inverse Fourier Transform of B10, block B5 contains the center 2K of the filtered signal and noise. The zero crossing algorithm (routine TEGULO) is applied to this block.

f. Block B7 - Contains the histogram, a function of frequency, generated by TEGULO.

g. Blocks B0', B1', B2' - Used for final equalization and averaging of the histogram block. The primes signify that these blocks are not defined and used until after all data has been analyzed in TEGULO. Block B0' is then the output block.

3. Data Input

The following sections describe the details of HISCAN. A representation of the major data flow and processing steps is contained in Fig 3. The data input portion occupies the upper blocks and is described as follows.

Sampled data is loaded into the 2048 word temporary storage block, B0, from either an analog to digital (A/D) converter or a data storage device such as a disk. This data is subsequently moved from block B0 to block B4 by an instruction MOVE B0,B4. the next input of data is read into B0 and moved to B9. At this point, 4K samples (words) of a time series have been placed into B8 for further processing starting with the direct fourier transform (DFT B8) shown in Fig 3. After the processing loops through TEGULO have been completed, the program returns to enter the next 2K samples. Since B0 still contains the last 2K samples associated with the loop just completed, this data is moved to B4. New samples are then read into B0 and moved to B9 for the next processing loop. As will be described later, this rather complex method of data input is necessary

to prevent the loss of data while allowing for the virtual elimination of end effects resulting from the digital processing.

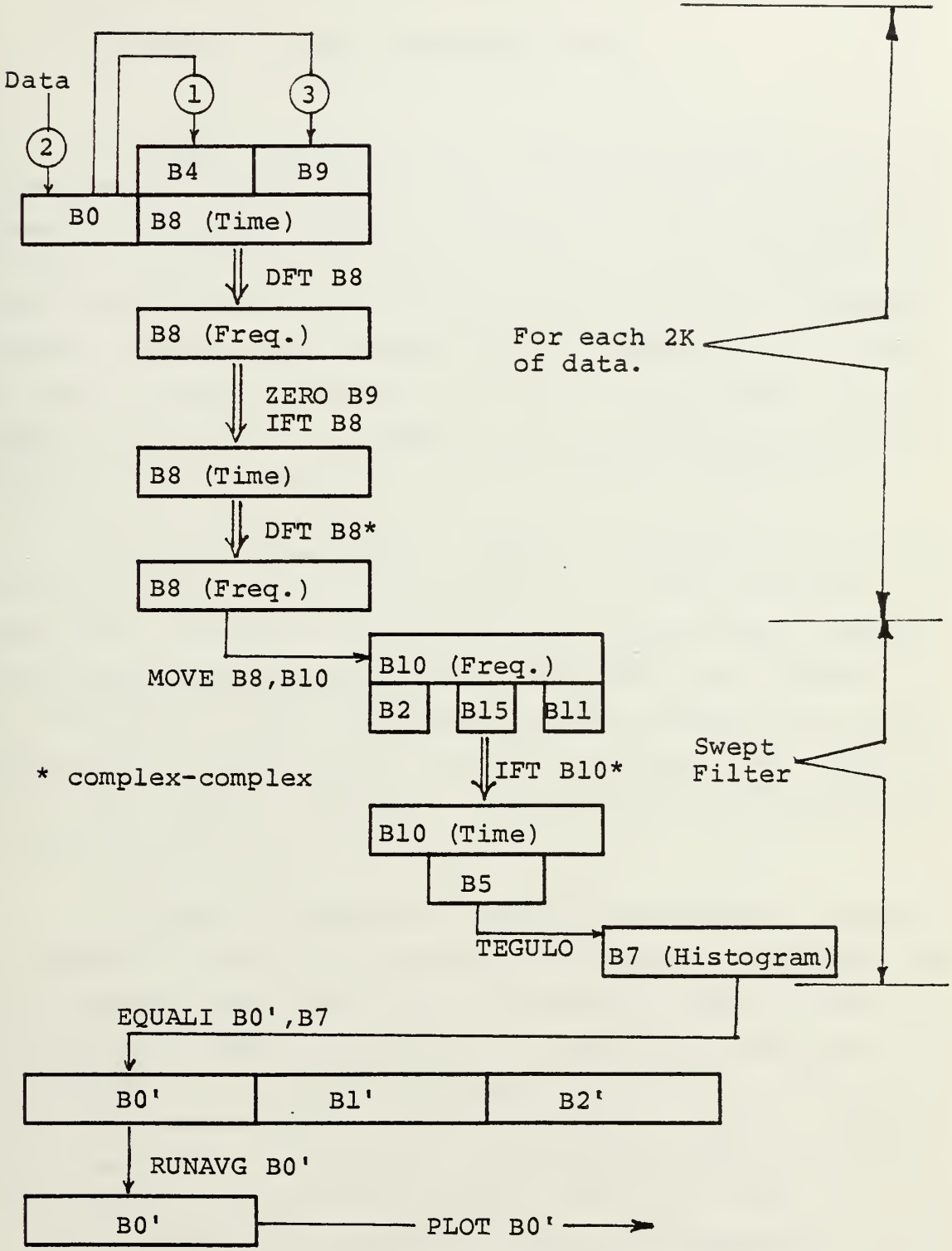

Figure 3 - FLOW CHART OF HISCAN

4. Transform to the Frequency Domain

Once the time series is loaded in to block B8, the corresponding frequency spectrum, consisting of 2048 complex elements, is computed using a hardware FFT microprocessor with the results stored back in block B8. At this point, an ideal filter is constructed by simply setting all frequency elements outside the desired filter bandpass equal to zero. The Inverse Fourier Transform (IFT) of this block is the ideally filtered time signal. This waveform is tegular in nature and can be analyzed by zero crossing techniques.

Because tegulometric methods require considerable numerical calculation and manipulation, it was necessary to search for methods to speed up the computational process. Since many of the time-consuming operations are related to the DFT-IFT routines, Professor Marmont modified the driver program of the hardware FFT device to store all required sine and cosine values in a table instead of using more lengthy interpolation.

A second significant increase resulted by reducing the number of operations necessary to compute a sequence of DFT, filter, and IFT. The algorithm used in the F4 microprocessor makes provision for computing either the real to complex or the complex to complex transform. The real to complex DFT performs the following general steps: complex fold, unscramble, and unfold. The corresponding IFT does a: fold, complex fold and unscramble. The final step of the DFT is to unfold the frequency components whereas the first step of the IFT is to perform the reverse operation of folding before proceeding. Since the analysis method uses the DFT/IFT to produce only a narrow band filtered time signal for zero crossing analysis, the fold-unfold steps

represent extra computational steps which Professor Marmont realized could be eliminated.

The complex to complex form of the DFT defines the time function as complex where the even words (the first sample is defined as the zero sample) and odd sample numbers as imaginary. The DFT then forms a complex fold, and unscramble with no unfolding. The complex to complex IFT then will accept the unfolded data, perform a complex fold, and unscramble to obtain the time function. This latter form of the DFT/IFT resulted in significant speed increases in that the real to complex takes 423.0 milliseconds while the complex to complex transform requires 359.3 milliseconds. Because the frequency components are not unfolded, however, it does increase the complexity of the filter.

5. Swept Filter

Because the basis for this method lies in frequency determination by measurement of the zero crossings of the narrow band filtered noise, this implies that the filter must be "moved" incrementally through the frequency block. The filter could be moved in steps such that it does not overlap with the previous setting. Although this results in lower computational requirements, it also results in a very poor frequency determination because:

a. The predominant frequency found by the zero crossing algorithm will be weighted toward the center frequency of the filter.

b. Strong frequencies within the filter passband will "pull" other frequencies toward the strong element.

c. Weak signals will be captured by strong signals within the filter band.

As a result of the above effects, the filter is "swept" through the range of interest, incrementing the filter location by one frequency element after each zero crossing frequency analysis. This tends to average the above effects and produce a linear frequency scale. Since the same DFT is used for an entire filter sweep, a copy is maintained in block B8 and moved to block B10 for successive filtering. Upon completion of the filter sweep across the frequencies of interest, a new set of time samples is read into B0 and B9 for the next filter and TEGULO cycle.

Since the DFT used for the filter is the result of a complex to complex cpmputation, the frequencies are not unfolded. As a result, the values for a specific frequency component, X(n) = Xr(n) + j Xi(n), are located in two addresses which are symmetric around the midpoint of the frequency block as shown in Fig 4. The first block depicts a real to complex DFT in which two frequencies X(n), low in the block, and X(m), high in the block, are located. A filter which detects the low frequency, X(n), would be constructed by setting all other elements outside the bandwidth to zero.

Because of the lack of unfolding in the complex to complex case, it is seen that location 1 is a combination of low frequency ,X(n), and high frequency,X(N-m); location 2 is a combination of X(m) and X(N-n). By necessity, the filter must be structured to allow both the X(n) and X(N-n) components through for the complex to complex IFT which follows. To prevent X(m) and X(N-m) from interfering in the IFT, the upper frequencies are set equal to zero by zeroing block B9 pricr to performing the complex to complex DFT. The resulting complex to complex IFT will then contain only the frequencies within the desired bandpass.

Although the complex to complex DFT filtering

requires setting all frequencies greater than X(N/2) equal to zero, where X(N) equals the maximum frequency in the real to complex DFT, it is still possible to analyze this higher block of frequency elements. By shifting the upper half of B8 to the lower half prior to zeroing block B9, the higher frequencies may be analyzed with no other effect on the programming.

Real to Complex DFT Filter

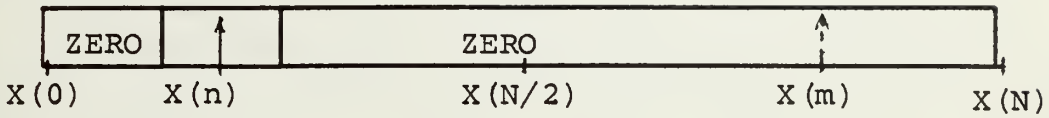

Complex to Complex DFT Filter

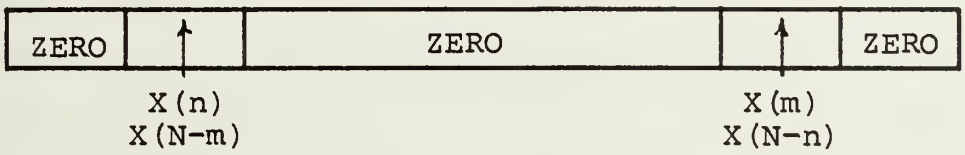

Complex to Complex Filter Formation

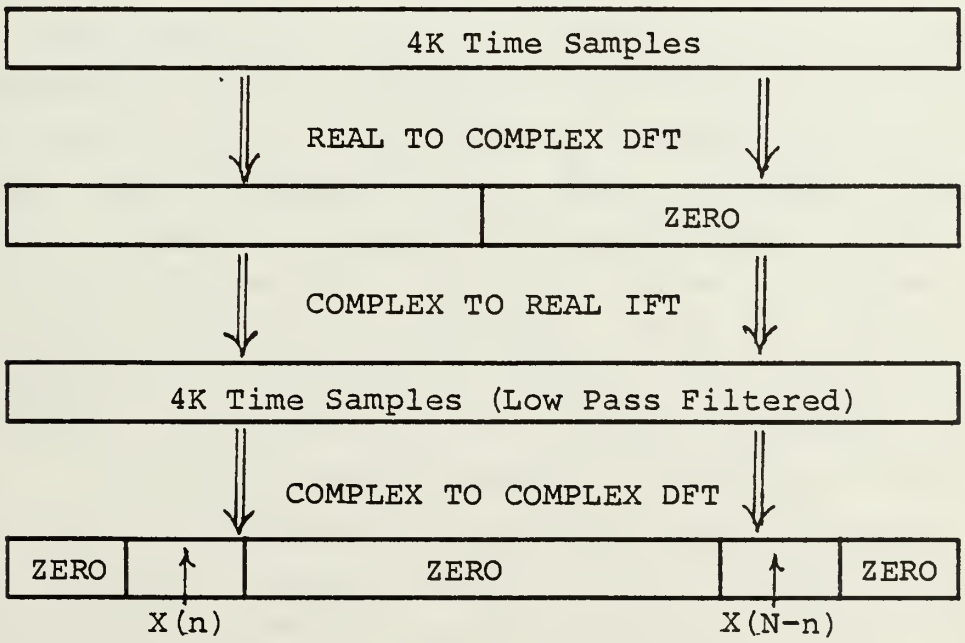

Figure 4 - FILTER CONSTRUCTION

6. Zero Crossing Algorithm Using TEGULO

The fundamental program for this analysis is the zero crossing measurement of frequency, computed in a routine called TEGULO. For each step in the filter sweep, TEGULO detects the sample point separation between seccessive negative to positive zero crossings. This separation is converted to frequency and the appropriate location of the histogram block is incremented by one. The histogram block is a 4K word block whose addresses are proportional to the frequencies determined by TEGULO. As the zero crossings are encounterd and the respective frequencies are measured and counted, the histogram block becomes a measure of the relative occurrence of the various frequencies.

The discrete fourier transform is a discrete representation of a continuous spectrum. If the Nyquist sample rate is always satisfied, all frequencies within the passband are represented by these discrete frequency elements. Since the narrowband filtered time signal will contain all frequencies within the filter, a higher degree of frequency resolution is possible. This is accomplished by performing an interpolation between the samples as though there are 2^{11} additional points between successive sample points. A typical sampled waveform is shown in Fig 5. It is seen that the negative to positive zero crossing pair occurrs between samples one and two and samples n and n+1. Since the negative value w_n and positive value w_{n+1} are known, the actual time of the zero crossing can be determined using similar triangle relations. This linear interpolation may be used if the maximum frequency analyzed is limited to some fraction of the maximum available in the DFT. In TEGULO, a compromise is made to limit the analysis

frequency such that there are a minimum of 10 samples per cycle. This allows for reasonable accuracy in the linear approximation. By counting the number of integer and fractional samples multiplied by the 2048 constructed points per sample interval, the frequency may be determined by the inverse relation between period and frequency. This value found is converted to a frequency address in the histogram such that there is an increase in frequency determination by a factor of 10. Then the histogram block, consisting of 4096 words, will represent 409.6 successive frequencies.

The ideal filtering results in distortion of the filtered time domain block because of convolution with the Sinc function which is the fourier transform of the filter aperture. Because of the reciprocal relation between frequency and time, a narrower filter implies greater distortion in the time domain. In HISCAN, the optimum filter has been found to be 10 frequency elements in width so that the zeroes of the Sinc function occur every 409.6 samples. This effect is primarily noticed at the ends of the time block. To minimize this end effect, only the center 2K of the filtered time data is analyzed for zero crossings.

The algorithm of TEGULO detects the first negative to positive zero crossing and defines this as the initial zero crossing so that there will be one less cycle counted in a given block than the total number of cycles. Reduction of end effects dictates that only half the IFT block should be analyzed by TEGULO so that the total number of cycles counted is 1/2 that of the frequency. As seen in the lower portion of Fig 5, which represents blocks B10 and TEGULO block B5, only four zero crossings out of the eight in B10 are available for counting. Since TEGULO marks the initial negative to positive zero crossing as the initial point, the analysis results in producing a final output of 3 counts.

Extension of this analysis to lower frequencies reveals that no counts will result for frequencies less than 4 Hz. Therefore, the histogram block is established to contain frequencies from 4.0 to 413.5 Hz. (It should be remembered that those frequency elements are "digital" frequency. The actual frequencies depend upon sample rate and any shifting of the DFT elements prior to TEGULO.)

Because phase reversals can occurr in the tegules, zero crossing analysis can produce frequency measurements which lie outside the filter setting. Since these frequencies are extraneous, TEGULO rejects all zero crossings outside the current filter setting and increments only those histogram frequency locations corresponding to the current passband.

Typical Sampled Waveform

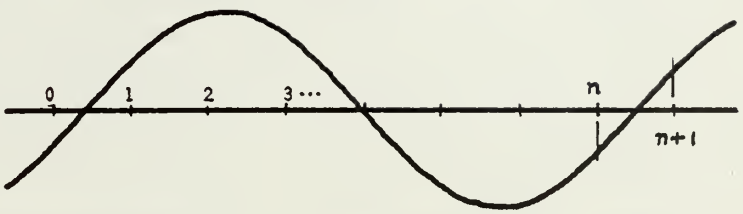

Linear Interpolation

n = sample number
w_n = value of waveform at point n
d = zero crossing to next sample point

$$d = 2048 \frac{w_{n+1}}{|w_n| + w_{n+1}}$$

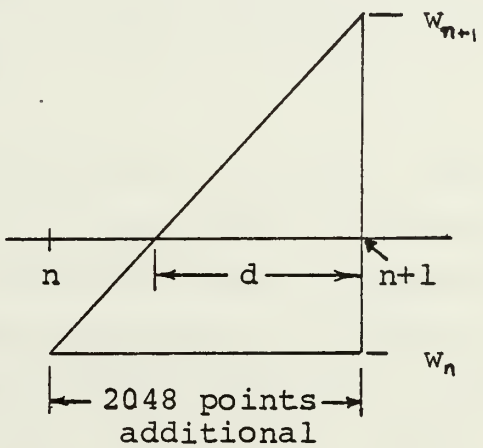

Zero Crossing Counts

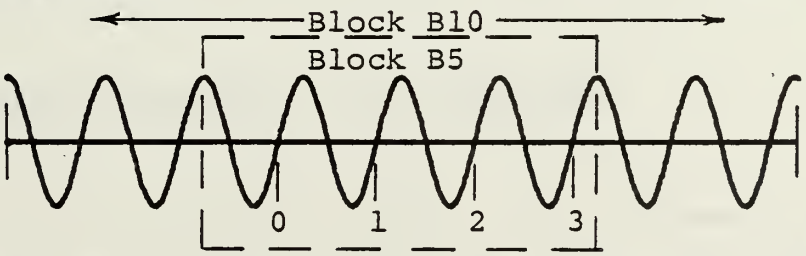

Figure 5 - ZERO CROSSING DETERMINATION

7. Equalization

After all data has been analyzed and the results placed in the histogram block, it becomes necessary to equalize the histogram data. In a given block of data, the number of zero crossings, hence the number of counts in the histogram, will be greater for a high frequency than a low frequency. A program, called EQUALI, multiplies each frequency dependent word in the histogram block by a scaling factor whose value decreases with increasing frequency. This results in a histogram whose amplitude is now a measure of the percentage of time that a frequency was observed during the analysis period.

If the total analysis period is short, there may be only a few counts in the unequalized histogram. To compensate for this and to allow for a readable plot, an additional arbitrary scaling multiplier is applied to all words of the block. Using a fixed multiplier, however, can lead to overscaling due to the potentially large dynamic range of this method. To preclude this from occurring, an overflow detection scheme was incorporated during this work to dynamically reduce the scaling multiplier when required.

8. Running Average of the Histogram

Prior to final display, it becomes necessary to smooth the equalized but highly irregular histogram. This irregularity results from two sources. A real signal will typically vary slightly in frequency over short time periods due to modulating effects of the transmission medium. This results in a spread of counts to adjacent frequency locations in the histogram and can reduce the detectability

of a signal in a fine-grained analysis. Additionally, at high "digital" frequencies, roundoff in the F4 FFT microprocessor and in zero crossing interpolation can result in placing frequency counts up to 5 histogram addresses from the actual frequency. This is not a significant loss in resolution since it is restricted to the upper frequencies analyzed by TEGULO and since the inherent accuracy of TEGULO is a factor of 10 greater than the parent DFT.

The equalized histogram is therefore smoothed in routine RUNAVG by adding successive and adjacent histogram words to produce a running average. The number of frequencies included in this running average can be varied with an external input parameter to the program. In addition, this routine scales the block to maximum numerical significance without producing overscaling (overflow) of the largest value in the histogram.

The final results appear as a smoothed histogram whose amplitudes, frequency dependent, are a measure of the probability density or persistence of each frequency. An example of a typical output is contained in Fig 6. Examination of Fig 6 shows two major characteristics of this type of analysis. The first is the appearance of capture valleys adjacent to the frequency component. The second shows that the signal will build upon the noise histogram value to produce a higher peak at the signal location.

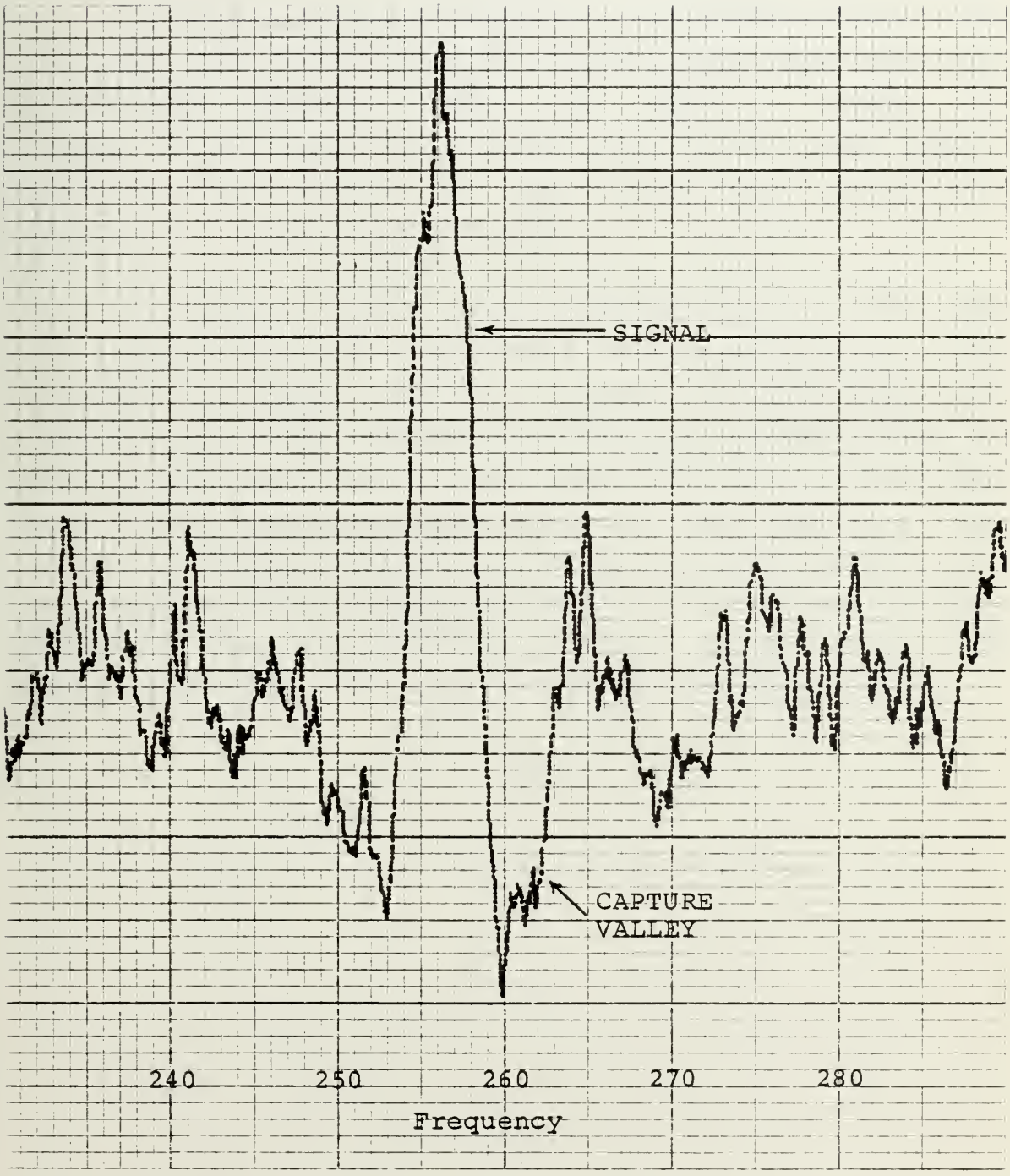

Figure 6 - SIGNAL IN WHITE GAUSSIAN NOISE

9. Continuity Of Data

It was seen in the section on on TEGULO that only one half of the filtered data in the time domain was used for the zero crossing analysis in order to reduce the effects of the narrow band ideal filter in the time domain. Unless care was taken in the data input this would have resulted in a loss of information.

To prevent such a loss, all data inputs were made via block B0 which is a temporary storage block seen on the flow chart of HISCAN. Before bringing in new data, B0, containing the last 2K samples from the previous frame, is moved to B4. New data is then loaded into B0 and B9 so that these blocks represent continuous data. This cycle is shown in Fig 7 where the numerals refer to the input samples and the letters refer to the central 2K filtered data analyzed by TEGULO. The bottom section of Fig 7 demonstrates that the analysis block, B5, does represent continuous data.

Data Input Scheme

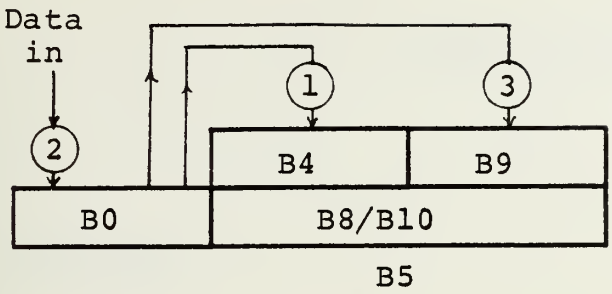

Relation of Input to TEGULO Data for Each Loop

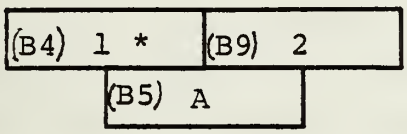

* Loaded into B4 from B0. B0 contains samples from previous loop.

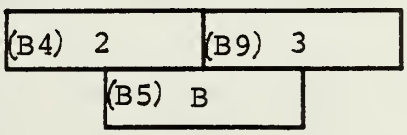

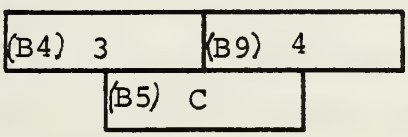

Relation of Input Data to TEGULO Analyzed Data

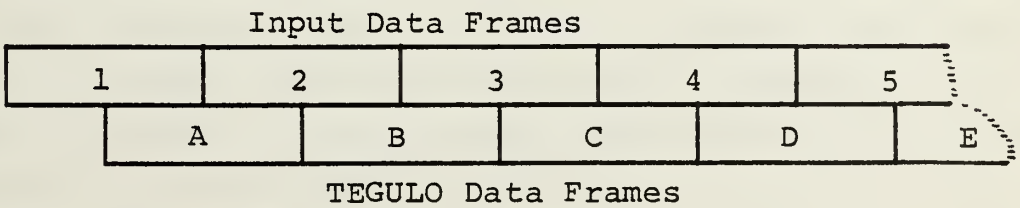

Figure 7 - CONTINUITY OF DATA

III. TEST OF THE METHOD

A. EQUIPMENT

1. Hardware

All tegulometric analysis methods were performed digitally. This resulted from the nature of the analysis method which requires complex but flexible data handling equipment. The following equipment was used in the present investigation.

a. Digital computer (PDP-11/40), a high speed 16 bit central processor with 32K words of core memory.

b. FPE4 fast fourier transform (FFT) hardware microprocessor manufactured by the Time/Data Corporation. This processor transforms a 4096 point time series to a spectral series in 589.0 milliseconds. The inverse fourier transform (IFT) is performed in the same time. Softwear support was provided by Time/Data and later entirely replaced by Professor Marmont to increase processor speed to 423.0 milliseconds for 4K of data. It should be noted that the FFT operates using integer arithmetic vice floating point. It keeps track of and adjusts the exponent for the block of data so that maximum significance of the integer (mantissa) is maintained in the data.

c. Disk Memory (RK11-D) manufactured by Digital Equipment Corporation, holding 1.2 million words per disk pack, was used for program and data storage.

d. Other equipment such as an X-Y plotter, a storage

oscilloscope, and various signal generators were used as required for data output and input.

d. analog to digital conversion utilized a high speed, 12 bit A/D converter. Selectable sample rates were highly accurate since the sample pulses were generated by a crystal controlled oscillator.

2. Softwear

a. Time Series Language (TSL)

The initial softwear was written in Time Series Language (TSL), a form of BASIC which was provided by Time/Data. TSL was specifically designed to manipulate blocks of data, to utilize the installed hardwear FFT microprocessor, and to display results on either an X-Y plotter or a memory oscilloscope. Although relatively easy to use, TSL was found to have a number of disadvantages, among which were slow speed, a lack of adequate flexibility, and inability to perform the specialized routines necessary for tegulometric analysis. As a result, dedicated machine language routines were linked to TSL to increase speed and program simplicity.

b. Language, APTEC

As more routines were writted in machine language and as the requirement for absolute control over program and data location in memory became pressing, all tegulometric programs were writted in machine language. This necessitated the development of input/output routines and general data handling routines previously used in TSL. Thus, a new operating system, called APTEC, was developed.

This system, developed by Professor Marmont, provided improved speed in the FFT, absolute control of program and data location, and control of the system monitor program of the Digital Equipment Corporation. Its greatest assets were great flexibility of programming and simplicity of use. This language is still under active expansion.

B. GENERAL APPROACH

In order to demonstrate the accuracy of the method and to measure improvements in sensitivity, it was obvious that input data had to be consistent from one computer run to the next. Since the major input was to be approximately white gaussian noise, a lengthy recording of noise was filtered with a fourth-order Butterworth filter, sampled in digital form at the Nyquist rate, and placed on a memory disk. Test signals were generated in softwear and also stored on the disk. Test programs read the noise and signal off the disk, scaled the signal to the desired signal to noise ratio, and added the scaled signal to the noise in the data input block, B0. The desired parameter control and reproducibility was achieved in this manner.

Two sets of noise were recorded with an A/D full scale setting of ≠ 1.0 volts. The first consisted of 60 2K samples at 0.24 volts rms with a filter setting of 100 Hz and a sample rate of 204.8 Hz. This corresponded to 10 minutes of actual data. The second sample contained 120 2K samples recorded at 0.24 volts rms with a filter setting of 2000 Hz and a sample rate of 4096.0 Hz. This represented one minute of data. The voltage levels were chosen to obtain maximum numerical significance of the noise data while reducing the probability of numerical overflow to a minimum.

Since both the signal and noise was in digital form, accurate measurement of the important noise parameters could be made. The first test consisted of checking for any overranging of the analog to digital conversion process in the recorded data. Of the 60 frames of 2048 samples per frame in the first sample, there were only 17 A/D overranges, no two of which were contiguous. The DC value was determined to be -30 (out of a total range of 32767). This corresponded to an analog voltage of 0.92 millivolts. Analysis of the second set of noise yielded similar results. From the standpoint of overflow and low DC, the test noise was judged as satisfactory. The digital form of the noise data was also analyzed to determine its root mean square value. This could have been computed by the averaged time interval of the noise squared over the time of sampling.

$$v(t)^2 = \frac{1}{T}\int_0^T [v(t)]^2 dt$$

Since the recorded noise was bandwidth limited to W Hz, the average noise power, N, could be computed by using the relationship:

$$N = \sum_{-TW}^{TW} c(n)c^*(n)$$

where $c(n)$ and $c^*(n)$ are the complex Fourier coefficients and their complex conjugates.

Further, it was assumed that the noise was gaussian with a zero mean so that the variance of the noise could be described as:

$$\sigma^2 = \overline{v(t)^2} - \overline{v(t)}^2 \qquad \text{but } \overline{v(t)} = 0$$

$$\sigma^2 = \overline{v(t)^2} = \sum_{-TW}^{TW} c(n)c^*(n)$$

Since the computer returns the Fourier series components a_n and b_n, the actual algorithm used to determine

the value of σ^2 was:

$$\sigma^2 = \frac{1}{M} \sum_{0}^{M-1} \left[\frac{1}{2} \sum_{0}^{N-1} (a_n^2 + b_n^2) \right]$$

where: M=total number of sample frames
N=total number of frequency elements per frame

The square root of this result is the rms value of the noise. To obtain the noise power per Hz, N:

$$N = \sigma^2/W$$

This technique permitted the determination of the noise power and rms value for any frequency range for signal to noise calculations.

C. TEST OF KEY ROUTINES

1. General

This section is devoted to the testing of the major and more complex routines used in the main program. Those routines not described here, but used in the analysis, such as moving data from block to block, performing square roots, defining data blocks, etc., were tested thoroughly in other work.

2. Swept Filter

The detailed structure of the complex to complex DFT form of the filter is shown in Fig 8. The set of numbers above the block describes the location of the frequency elements. The numbers below the block represent consecutive

complex element numbers and those within the block the consecutive word numbers in memory. It is seen that element number 3 contains the data for frequencies 3 and 2045. Its symmetric element location high in core is number 2045. Prior to forming the complex to complex DFT, all frequencies above 1024 were set equal to zero so that the filter shown in Fig 8 would allow only frequencies 3,4, and 5 to appear in the IFT.

The logic which determined the location and size of filter blocks B2, B11, and B15 was verified in a test run. Additionally, a time domain test signal of 256 Hz was input, the filter set at 256 (no sweep) with the bandwidth set to one element, and the IFT examined. The IFT showed a cosine wave of 256 Hz with no distortion.

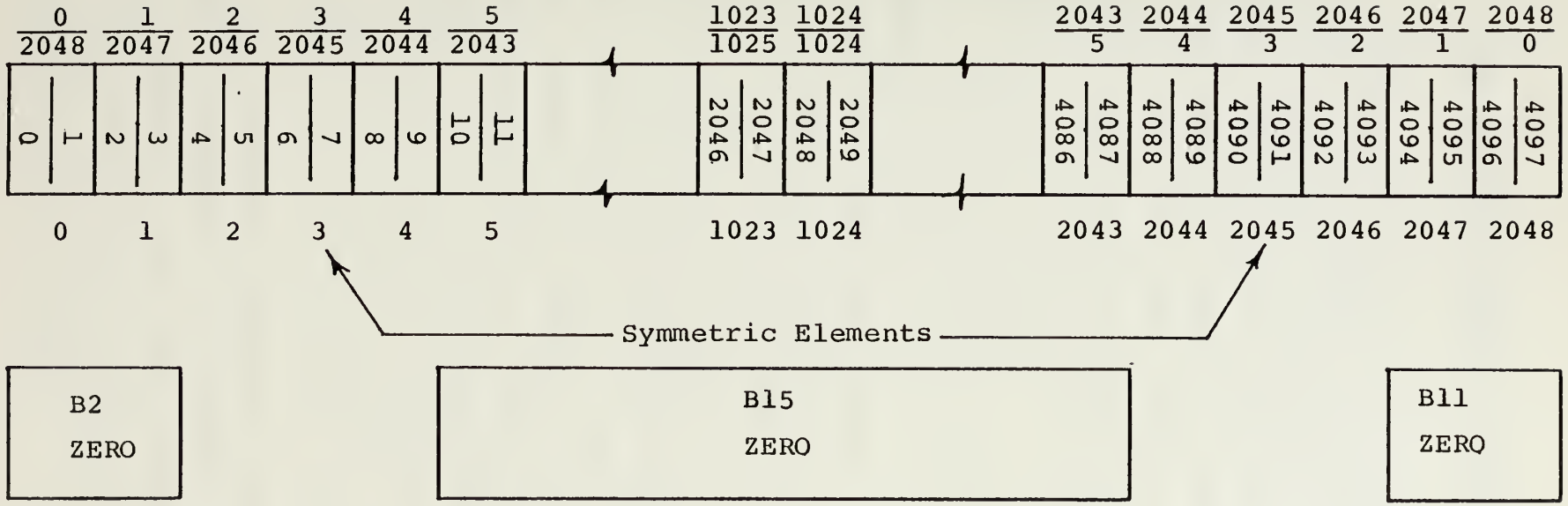

Notes: 1. Upper numbers indicate combined frequency elements.
2. Lower numbers describe complex element numbers (sequential).
3. Numbers within blocks indicate sequential word number within memory.

Figure 8 - SWEPT FILTER CONSTRUCTION

3. Zero Crossing Routine, TEGULO

TEGULO was tested for accuracy of zero crossing measurement, for accuracy of conversion from zero crossing spacing to frequency, for adequacy of the logic to exclude extraneous frequencies, and for prevention of overflow. The first test inserted a number of discrete frequency elements into the DFT block after setting the block equal to zero. The filter was allowed to sweep from frequency element 4 to 406 with a bandwidth of one element. The results in the histogram block showed that:

a. Frequency elements below 320 Hz were counted accurately and placed in the correct frequency location in the histogram block.

b. At the higher frequencies, the correct number of zero crossings were counted but some of the counts were placed in histogram locations adjacent to the proper histogram site. The worst case condition occurred for 320 Hz for which 950 counts appeared at location 319.9, and 320 counts at both locations 320.0 and 320.1. The sum agreed with the theoretical total of 1590 counts. The effect is believed caused by roundoff in the linear interpolation of frequency corresponding to a zero crossing pair. This was determined to be of neglible importance since the problem was restricted to the high histogram frequencies and since the routine, running average, effectively added the separated counts prior to final output.

The spurious frequency elimination logic was tested by fixing the filter at a single center frequency with various bandwidths and then analyzing the histogram data. This examination revealed that frequency counts appeared only within the filter bandwidth ≠5 histogram elements (≠ 1/2 DFT elements) as required.

In the white, gaussian noise samples tested, it was seen that the histogram counts were fairly uniformly distributed through the block and low in numerical value. The presence of a strong signal, however, could result in a large number of counts in the signal histogram location. In a lengthy analysis, this could have resulted in overflow of the histogram. To preclude overflow, logic was added to prevent any histogram location from exceeding the maximum value of 32767 (77777, octal). This was tested by counting a 256 Hz signal and observing the buildup in counts in the histogram. The maximum value was achieved as expected and no overflow resulted. Because EQUALI and RUNAVG both scaled the histogram data based on the largest value in the block, a very strong signal, counted in double precision, would result in a small scaling factor. This in turn would reduce the smaller variations in the histogram to the point where small signals could not be detected. This scheme therefore had the additional advantage of limiting the effect of strong signals when searching for weak signals in noise.

4. Equalization of the Histogram

The test consisted of loading the histogram block with the theoretical counts corresponding to each frequency. After equalization with EQUALI, the data in all locations should have been equal if roundoff was neglected. As expected, frequencies 1 through 20 of the 406 in the histogram were low by about 15 percent. This was not due to the inaccuracy of TEGULO but a reflection of the large scaling necessary to increase the small number of low frequency zero crossing counts to a large number using 16 binary bits.

This effect was not considered a significant problem because:

a. Analysis of actual data will normally occur over many frames of input data. This allows the counts, low in the histogram, to build up to a value where the integer arithmatic of the computer has only a minor influence.

b. The effect is limited to only a small part of the final histogram and appears as a minor reduction of the low frequency amplitudes. Since detection depends upon the relative heights of the histogram, a signal will still show up as more persistent than the neighboring frequencies.

The errors discussed in these last two sections were found to have no effect on the bulk of the final histogram outputs. The midrange from about 20 to about 300 Hz was accurate in frequency and amplitude to within one percent. From 300 to 406, the highest element, the amplitudes were within 0.2 percent.

5. Continuity of Filtered Data

It was asserted in the initial descriptions that end effects in the time domain, due to the ideal filtering, could be reduced in the Tegulo block, B5, by discarding the first and last 1024 samples in the analysis block by TEGULO. By careful input of data it was also possible to process without loss of data. In order to evaluate this, HISCAN was modified to plot the filtered time domain signal and noise instead of computing the histogram. This program, called TEGPLT, was run over successive frames of input data at a constant filter setting. It was found that the filtered data was indeed continuous from one frame to the next with no discontinuities in the data. This test was performed over a wide range of data and filter settings. It was noted that small distortions did appear if the bandwidth of the filter was reduced much below 6 elements. This effect was expected since narrowing the filter expands the effect in

the time domain.

From this it was concluded that the data used by TEGULO was essentially free from effects normally associated with sampling and ideal filtering using the discrete Fourier transform. An example of this is seen in Fig 9. The breaks in the graph between data frames are an artifact of the plotting routine and not an indication of a problem in the data.

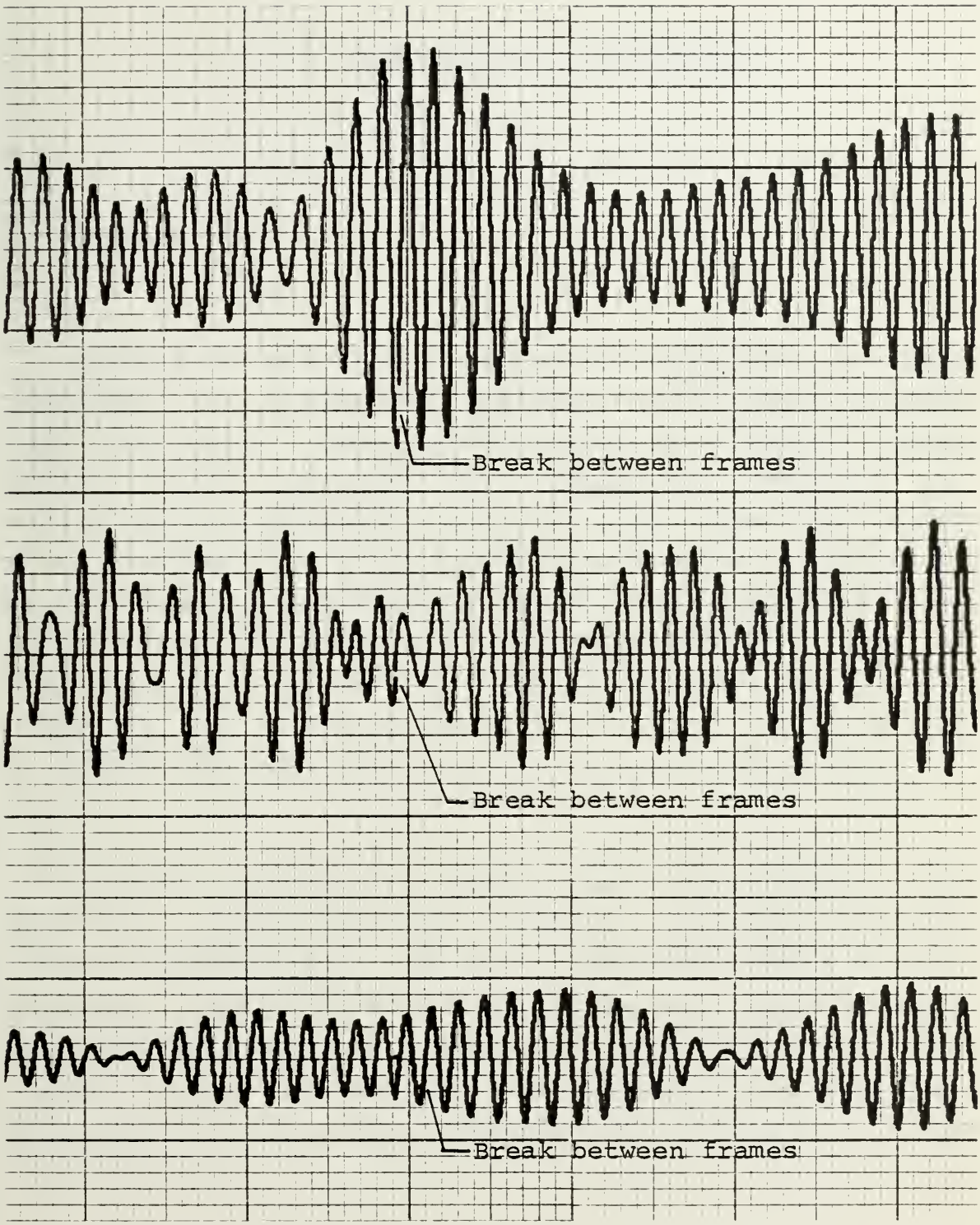

Figure 9 - CONTINUITY OF DATA TEST

IV. IMPROVEMENT OF SENSITIVITY

A. GENERAL

Because the method of zero crossing analysis is highly non-linear, the fundamental approach was experimental rather than theoretical. Using current theory as a guide, various schemes were selected as having the potential for sensitivity improvements. Since the test noise and signal were recorded on the disk, the input data was constant for each computer run. Any improvements in detectibility could be related to the method and parameters used.

B. ZERO INSERTION REMOVAL

Initial versions of HISCAN used time domain zero insertion. Zero insertion, however, was found to produce artifact frequencies in the DFT. Since this method depended strongly upon narrow-band filtering and zero crossing analysis, this resulted in potential distortion of the final output. After removal of the zero insertion, tests with sinusoidal signals showed significant improvement in the histogram data.

C. FREQUENCY COMPONENT LIMITING

It was found that a typical DFT of noise contained a number of strong frequency elements. If any strong frequency was within the filter bandwidth of a weak signal, the signal was "captured" and possibly would not appear in the filtered time representation. To alleviate this situation, the effect of limiting the magnitude of both very high and very low frequency elements in the initial DFT was investigated.

A program, called SLICE, computed the magnitude of each DFT element and modified those frequencies whose magnitudes exceeded either a preset maximum or minimum limit. This is shown in Fig 10 which depicts a DFT block and the two SLICE. levels. The upper or LIMIT level represents the cutoff of those frequencies whose magnitudes are very large. Values exceeding the LIMIT level were either set equal to zero or their complex components were scaled so that their magnitude equalled the LIMIT level without affecting the phase. The lower or CLIP level represents those frequency elements which are due entirely to noise. The complex frequency elements below the CLIP level were set equal to zero.

This method suffered from a major difficulty in that the actual magnitude of the signal element plus noise had to be known in order to set the levels involved. Since only the fact that a signal was present within a band of frequencies was assumed, no apriori knowledge as to its level could be used. If these levels were incorrectly set, a strong signal could be either removed or its effect reduced. A very weak signal, which adds coherently to the noise, could combine with the noise such that the final magnitude was below the CLIP level and thus be lost.

Despite these obvious problems, testing of the method was still fearlessly accomplished. The SLICE levels were

set such that the signal element magnitude was always within the SLICE band and therefore not modified. With a signal to noise ratio of -18.0 db, based on a noise bandwidth of one hertz, little or no improvement in the detectability was seen.

Because of the difficulties described above in setting the SLICE levels, a third method, called WHITEN, was developed. As seen in the third graph of Fig 10, all frequency elements were set to a single magnitude level. All scaling was accomplished so that the phase relations were unaffected by the magnitude change. Tests of this method also indicated a lack of significant improvement.

It was concluded that this method had little value at this point in the development of Tegulometric Analysis. It may be possible, however, that future tests with real data containing known interference sources may yet show that similar techniques are useful.

General Scheme

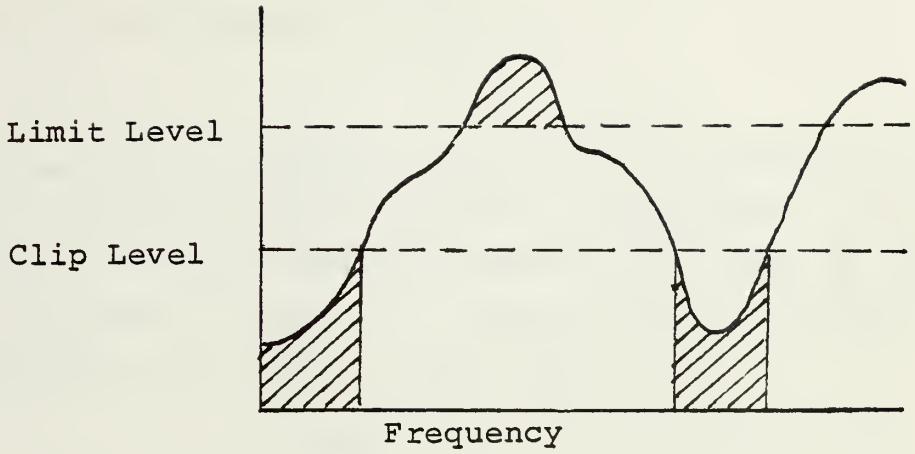

SLICE

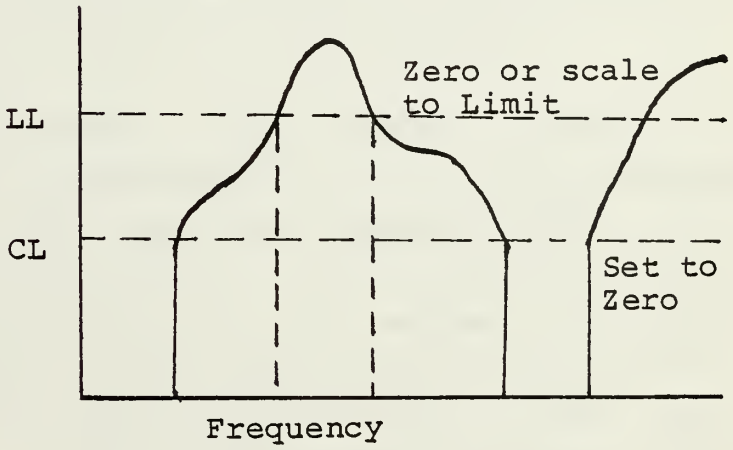

WHITEN

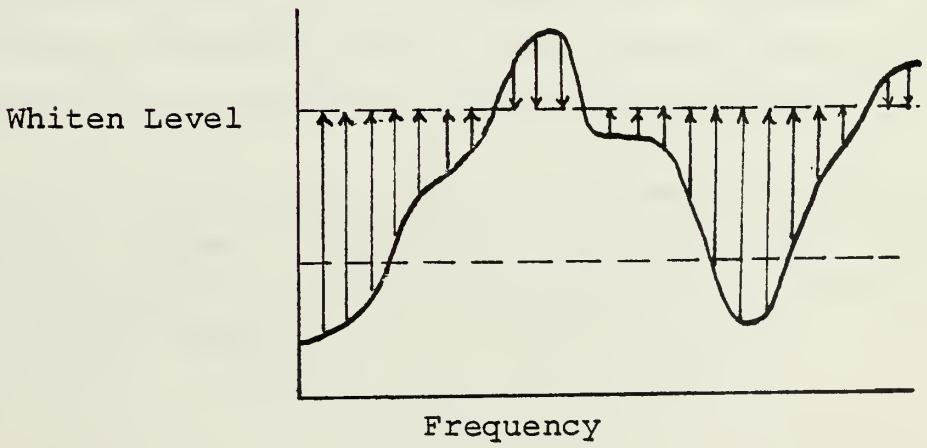

Figure 10 - FREQUENCY COMPONENT LIMITING SCHEMES

D. AVERAGING IN THE FREQUENCY DOMAIN

A proven method in reducing the effects of random noise is to average successive direct Fourier transforms. With gaussian noise, each frequency component will have an rms value, σ , and a mean of zero. If there are M averages, then the resulting rms value $\overline{\sigma}$ will be:

$$\overline{\sigma} = \sigma/\sqrt{M}$$

The rms of the signal will not be changed by the average so that potential signal to noise would be improved.

A modified form of HISCAN, called RUSCAN, (running DFT average with HISCAN) was developed to take running averages of the DFT and analyze the resulting frequency block. This modification is shown in Fig 11. Input data is read into block B0 and moved to B8 in the same manner as HISCAN. After DFT B8 and ZERO B9, the lower half of B8 is added to B6, which contains the current running sum of the direct fourier transforms. After initial memory load, the oldest DFT is subtracted from B6 and the newest DFT replaces the old data in the DFT memory blocks. The current averaged DFT is moved into B8 and processing continues as in HISCAN.

Results of the averaging technique showed a significant improvement in signal detection. Signals that were previously distinguished with difficulty at -18 db could be easily seen on the histogram.

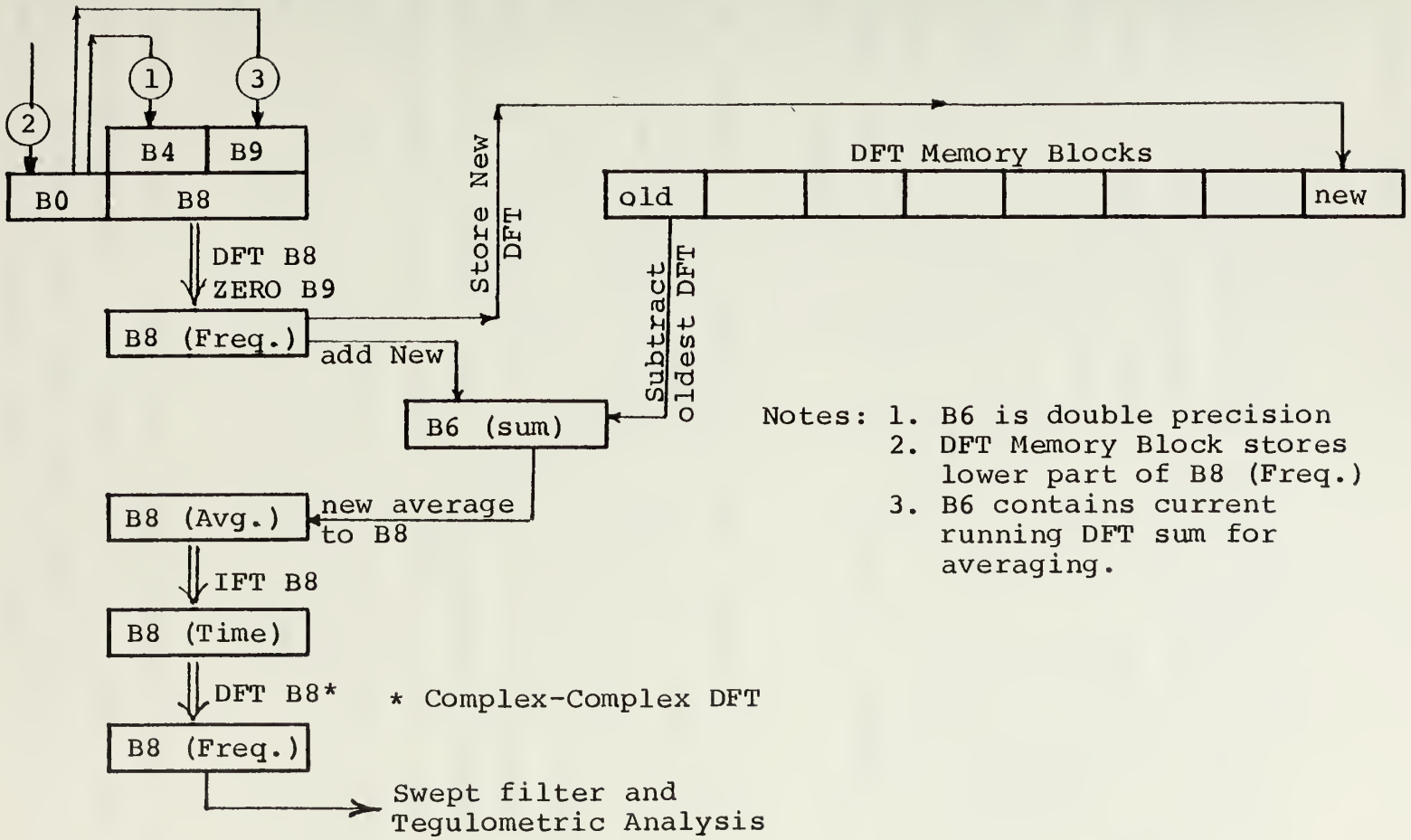

Figure 11 - MODIFICATION TO HISCAN FLOWCHART FOR RUSCAN

E. SHAPED FILTER FUNCTION

Observations of plotted data showed that the frequency of weak signals tended to be pulled toward stronger elements within the filter bandpass. This resulted in a dispersion of weak frequency counts in the histogram block. To counteract this phenomenon, a shaped filter function in the form shown in Fig 12 was tested. This triangular filter was applied to the DFT elements before the filtered IFT. In this, each frequency element is reduced in magnitude proportional to its separation from the center frequency, becoming zero at the 1/2 bandwidth separation from the center frequency.

A number of advantages were forseen by the triangular window. First, its transform, the Sinc squared function, should have produced lower effects in the time domain because the sidelobes are more quickly reduced than the Sinc pulse. Secondly, this filter should have accentuated the tendency of this method to count the frequencies in the center of the filter. Thus, the frequency pulling effect of strong signals on weak signals should have been reduced. Finally, for a triangular filter of twice the width of a square filter, the noise power would still be lower since power is proportional to the square of the element magnitude.

Despite high hopes, the test results were inconclusive in that improvement was noted in some runs but not in others. Because some improvement was noted, it is felt that investigation of shaped filters in future work is warranted.

Rectangular Filter

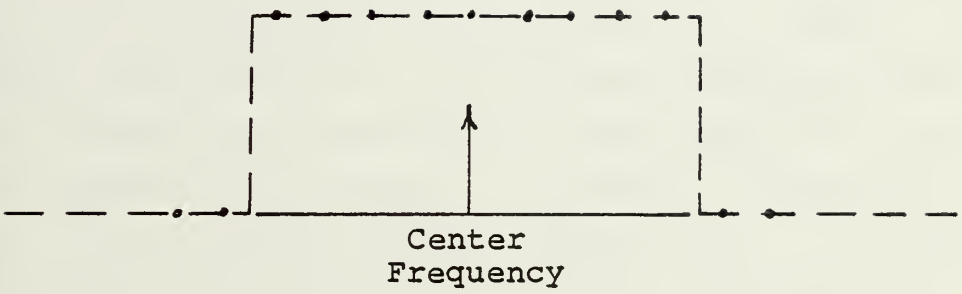

Triangular Filter

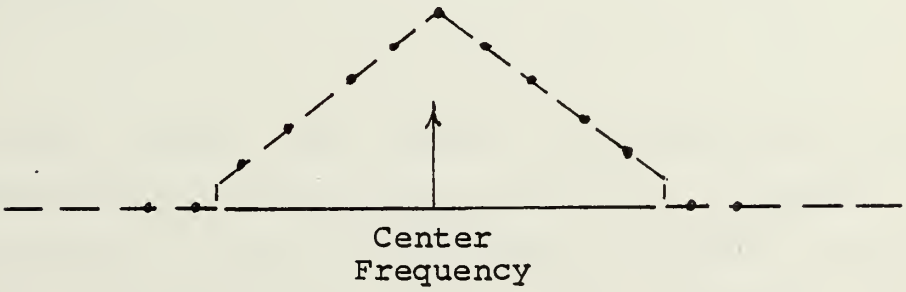

Figure 12 - FILTER SHAPES

F. FREQUENCY SHIFTING

In forming the complex to complex DFT, the upper half of the DFT frequency elements were set equal to zero making them normally unavailable for analysis. Further, the increase in frequency determination in TEGULO placed additional restrictions on the frequency analysis range. If greater accuracy was desired, the scan range had to be even further reduced to 20 to 300 Hz (digital frequency). To obviate this rather severe restriction, an additional feature was placed in the program after the initial DFT B8. This step allowed translation of any band of frequency elements into the section of the DFT over which the swept filter and TEGULO operated. This relatively simple modification allowed any frequency, within the range of the parent DFT, to be accurately examined. Tests showed this technique to be valid.

G. RESAMPLING

A final method was tested and shown to be of value. Since tegulometric analysis works best on a constant sweep filter bandwidth of about 10 frequency elements, improvement in signal detectability should have resulted from the reduction of the noise power per frequency element. Just such a reduction may be achieved by filtering and resampling as described below.

Consider that the data is sampled and handled as in HISCAN and as shown in Fig 13. If after the DFT, the upper three quarters of the block is set equal to zero and the IFT

performed, the resulting time signal will be oversampled by a factor of four. To match the sample rate with the new baseband limit, the extra data points may be neglected with no loss of information. In this case, every fourth word is moved to another block and placed in memory.

Assuming white gaussian noise, where the noise power spectral density is constant over the bandwidth, the original noise power, σ^2 , is reduced by a factor of four by filtering the upper three quarters of the d/fT block. the resulting filtered noise power, σ_f^2 , is:

$$\sigma_f^2 = \sigma^2$$

When the noise is resampled, this matches the sample rate to that of the filter so that the total period of a 4096 word block now represents 4 times the amount of time as the original data. The average noise power, σ_r^2 , in this additional, 4T, time period is the same as the original noise by:

$$\sigma_r^2 = \frac{1}{4T}\int_0^T [v(t)]^2 \, dt$$

Where is the value of the waveform amplitude at time,t. This additional time, however, results in four times the number of frequency elements over the same bandwidth W/4. This effectively reduces the average noise power per frequency element by a factor of four. Tests of noise show that this technique is valid and produced a reduction in the root mean square of the noise of 2.05 compared to the theoretical value of 2.0. Resampling by filtering the upper half of the DFT block and saving every other sample showed similar results.

Simple resampling precluded analysis of the upper frequencies in the DFT. An addition to the resample program provided for shifting the upper frequencies to the lower portion of the DFT block prior to actual resampling. In

this technique, the lowest frequency of interest was shifted to element one in the DFT block and element zero (DC location) was set equal to zero. Finally, the upper portion of the DFT block was cleared, the IFT taken, and the resulting time series resampled. Tests of frequency shifting and resampling validated this concept.

RESAMPLE Data Flow

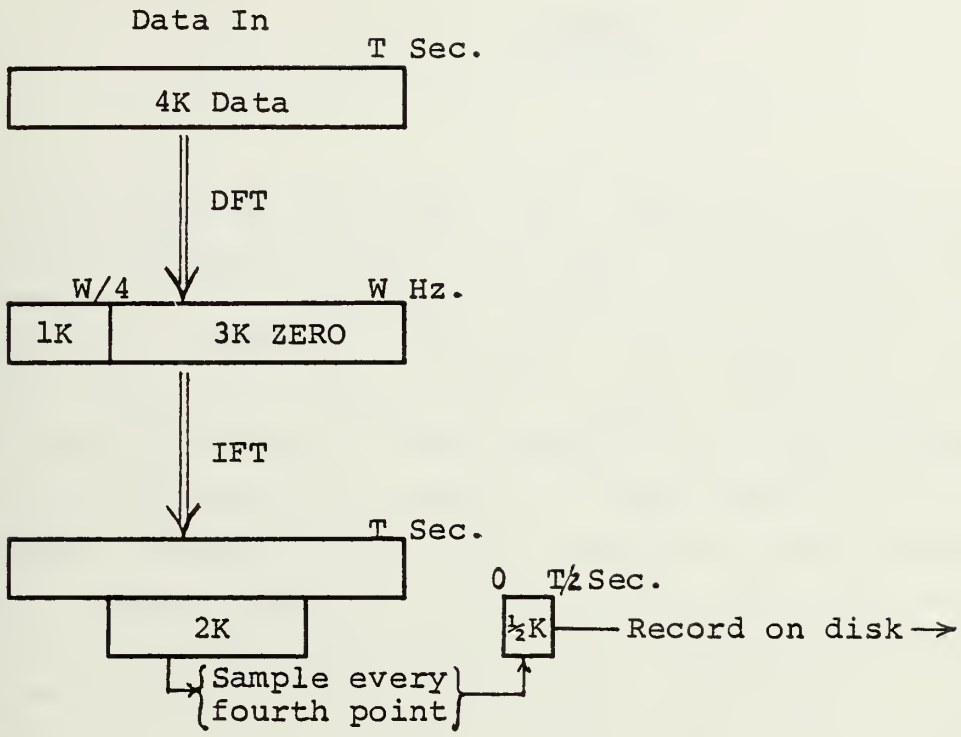

HISCAN Analysis After Resampling

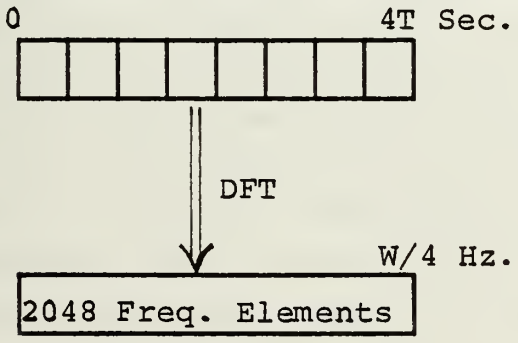

Figure 13 - RESAMPLE LOGIC

V. RESULTS

A final set of data runs was completed, incorporating the most promising signal enhancement techniques which were determined to be: resampling, running DFT averaging before HISCAN, and frequency shifting. A comparison was made between the signal in noise and a signal in resampled noise with varying numbers of DFT averages and varying numbers of input data frames. To perform these tests, a softwear generated signal of 1600 Hz, scaled to the appropriate signal to noise ratio, was added to the noise in the time domain. All frequency shifts during resampling and analysis were made such that the signal always appeared at frequency element 256 in the final histogram for ease of analysis. All histogram plotting was performed at 100 histogram points per inch. The averaged DFT plots were completed at 10 points per inch. In the graphs that follow, the upper row of numbers below the histogram refer to frequency. The lower row of numbers refer to the frequency element number in the DFT after any shifting. Because the significance of the histogram lies in the comparison of the relative heights of the frequency elements, no units are assigned to the vertical scale. Additionally, each signal plus noise observation was matched with an analysis with the same noise but no signal in order to provide direct comparison of signal enhancement. All data runs included were conducted with a rectangular window, 10 frequency elements wide.

Figures 14 and 15 show the results of analyzing 44 2K word frames of input data with no averaging or resampling. Since the initial sample rate was 4096 Hz, this corresponded to a total time sample of 22 seconds. The data of figure 14

contains a signal at element 256 corresponding to a frequency of 1600 Hz with a signal to noise ratio of -18.5 db. Figure 15 contains the same noise over the same time but with no signal. Comparison of the two graphs at the signal location shows only a small change due to the low level signal.

The next set of results, shown on Figures 16 and 17, was obtained by performing 6 DFT averages for each histogram computation by TEGULO over the same 44 frames as the previous figures. Comparison of Fig. 16, containing the -18.5 db signal, with Fig. 17 shows that the region around the signal has increased in value. This change, although small, is greater than in the previous figures. The region immediately adjacent to the signal is higher in level than for no signal by about 8 percent. Beyond this region but within the 10 element filter bandwidth, the counts are depressed.

Figures 18 and 19 are the results of analyzing 11 frames of resampled noise with no DFT averaging. Because of resampling, this corresponds to 44 frames of original data. As in the previous figures, an increase in the counts at the signal location is seen. However, the precision of frequency determination has been significantly improved because of both the inherent increase in accuracy by a factor of 4 due to resampling, and an apparent lower amount of dispersion of signal frequency counts in the histogram.

Figures 20 and 21 are the histograms for 11 frames of resampled data (44 frames of original data) in which 6 DFT averages were completed for each HISCAN swept filter analysis by TEGULO. Dramatic improvement in the signal detectability may be seen by comparing Fig. 20 which contains the -18.5 db signal and Fig. 21 which is for the noise alone. It should be noted that the accuracy of the

frequency determination in this plot is about 40 times greater than the original DFT which is limited by the relation of 1/T, where T is the sample period. Additionally, the method was able to discriminate between the 256.00 signal and the noise frequency element at 256.25 Hz. The capture valleys on either side of the signal are prominent, indicating the shift of counts in the histogram to the frequency spike. Measurement of the area under the curve indicates that the area with and without signal was approximately constant over twice the bandwidth centered on the signal. An increase in counts due to the addition of a signal is compensated for by a decrease in histogram counts adjacent to the signal and within the bandwidth of the filter. Since the output histogram is a measure of the signal and noise frequency probability distribution function, this result is reasonable.

The next analysis was conducted on 11 frames of the resampled noise using 10 DFT averages but one HISCAN. Figures 22 and 23 display the results. Although the signal is seen, the accuracy of its determination is not as good as in the previous figures. This effect is typical of the process and indicates that there may be an optimum value of DFT averages and HISCANS. The next series of graphs represent analysis of 21 frames of resampled signal plus noise and noise alone. This corresponds to 84 frames of original data and 42 seconds of time for a sampling rate of 4096 Hz. Figures 24 and 25 resulted from HISCAN analysis with no DFT averaging. Figures 26 and 27 resulted from performing 6 DFT averages for each of the 15 HISCAN analyses. The number of averages was increased to 10 DFT averages per HISCAN and the results are contained in Figures 28 and 29. In comparing these last four figures, it is seen that the signal appears slightly stronger for the 6 averages per HISCAN. Additionally, comparing Fig. 26 and 27 with Fig. 20 and 21, which were derived from about half the

number of data frames, little signal detection improvement is observed in the longer runs. This seems to imply that there is an optimum number of HISCANS for each output histogram. The fact that tegulometric analysis produces results within a short time period implies that this technique has application as a detection scheme where time is an important consideration. In this case, signal detection could occur in 22 seconds of data at a signal to noise ratio of -18.5 db. From the results to date, the optimum combination appears to be 44 frames of data, resampled by a factor of 4 and analyzed with a 6 running DFT average per each of the 5 HISCAN sweeps. Frequency shifting to permit analysis of all DFT frequencies was also validated.

A final comparison was made with the averaged DFT over the same 44 frames of data with no resampling. The resulting magnitude plot is contained in Figures 30 and 31. Since the DFT has 1/10 the frequency resolution as HISCAN, the averaged DFT plots appear far more discrete. As in the histograms, the signal was placed at element 256 for convenience. Although the signal appears to be quite prominent, examination of the entire DFT block revealed that it was only one of many other stronger frequency elements. Because the test signal had an even number of cycles in the time window, the DFT did not suffer from any leakage effects. For a real signal, however, it is expected that there will not only be leakage in the DFT but also will be modulation of the signal by the transmission medium. This would most certainly reduce the magnitude of the signal in the averaged DFT. Because tegulometric analysis takes into account signal frequency variation and because of the greater accuracy of frequency determination, this method is not expected to be as degraded when real signals and noise are analyzed. This conjecture was affirmed by the work of T. J. Colyer in which acoustic data was analyzed without

resampling, DFT averaging, or frequency shifting. This simpler form of HISCAN, which was found to be appreciably more sensitive than conventional DFT methods, was more appropriate since the acoustic signals were an order of magnitude stronger than those used in this paper. More complex methods, including DFT averaging and resampling, would not have significantly improved the analysis results.

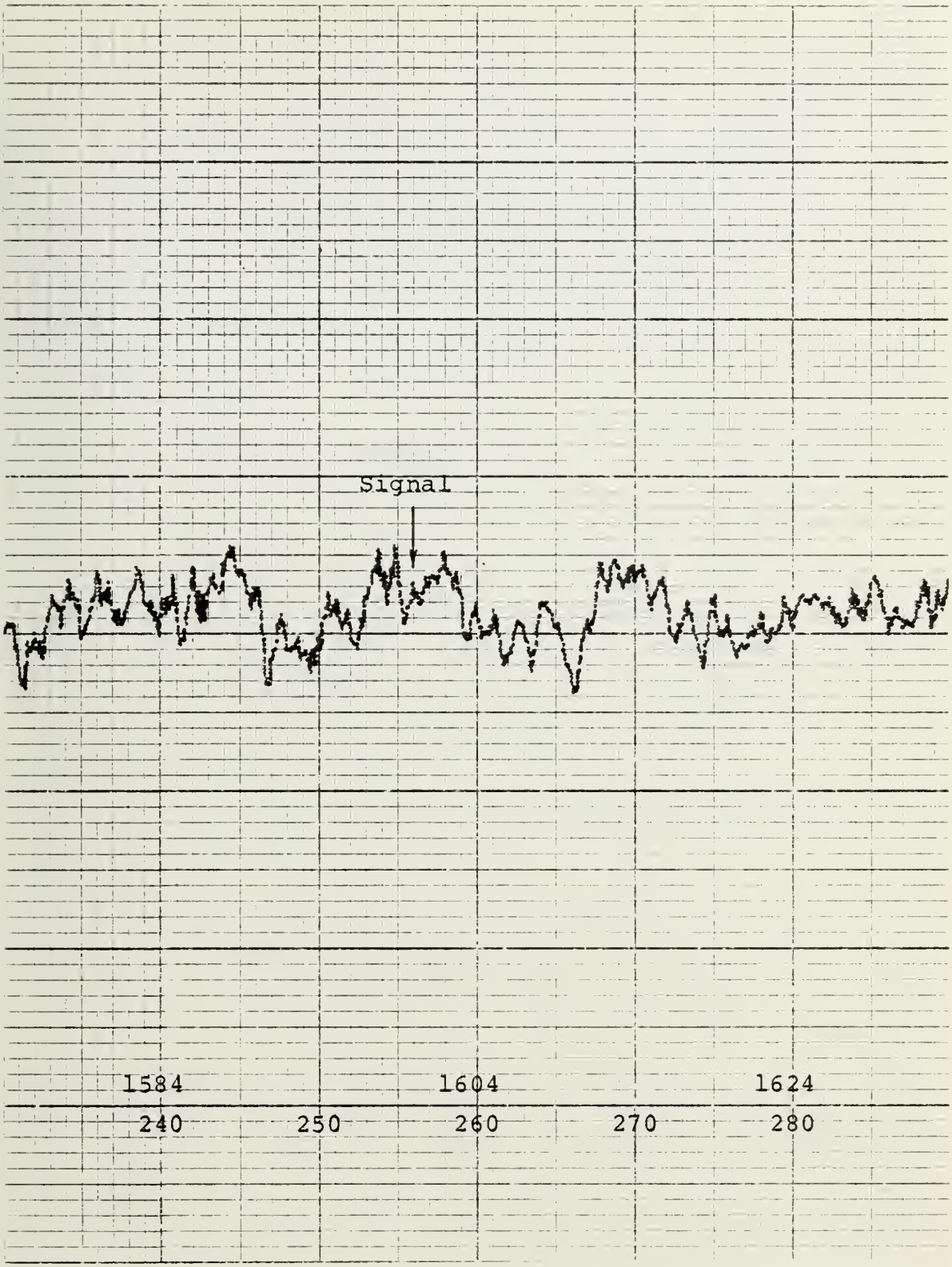

Figure 14 - SIGNAL PLUS NOISE, NO AVERAGE, 44 FRAMES

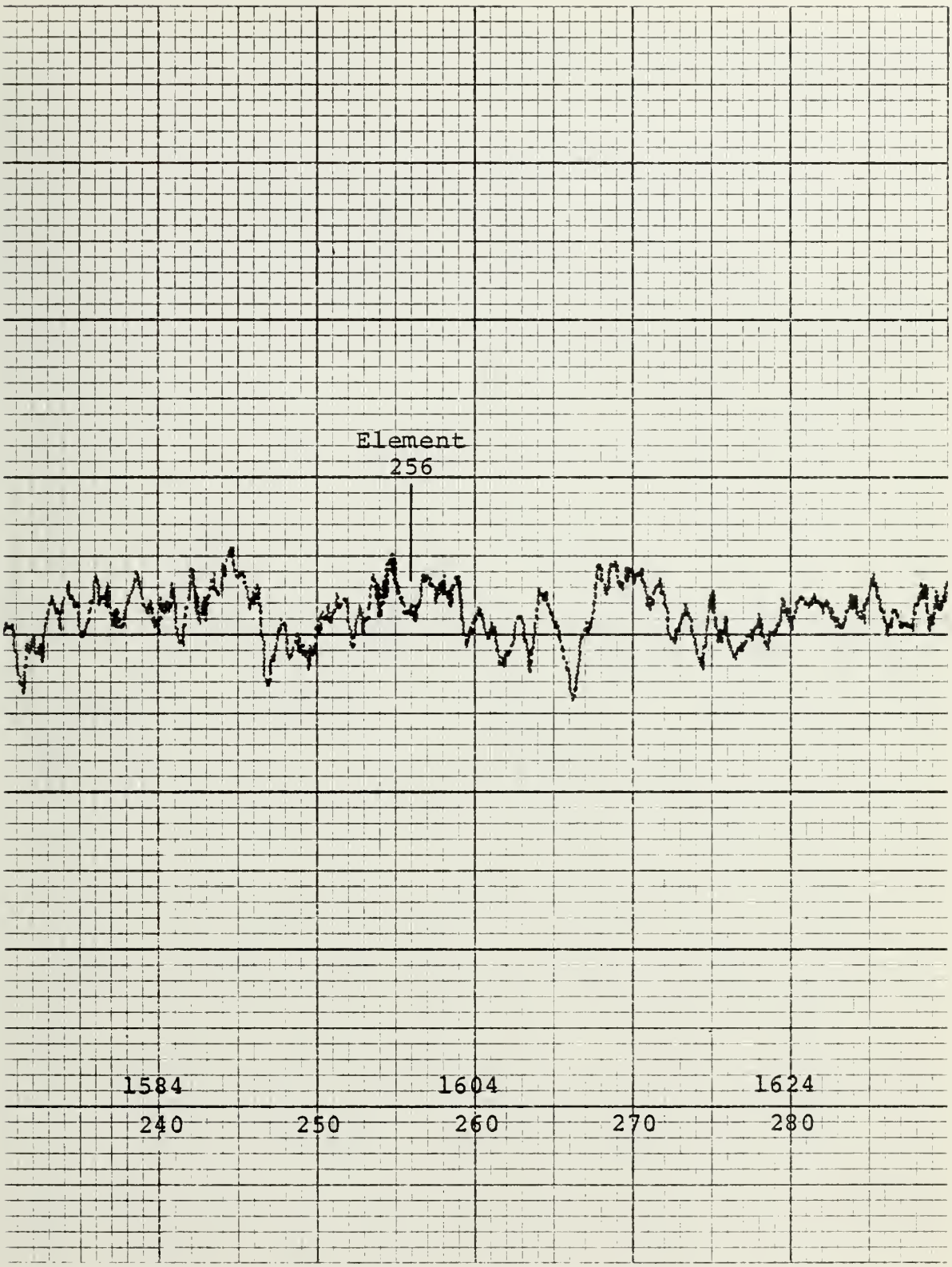

Figure 15 - NOISE, NO AVERAGE, 44 FRAMES

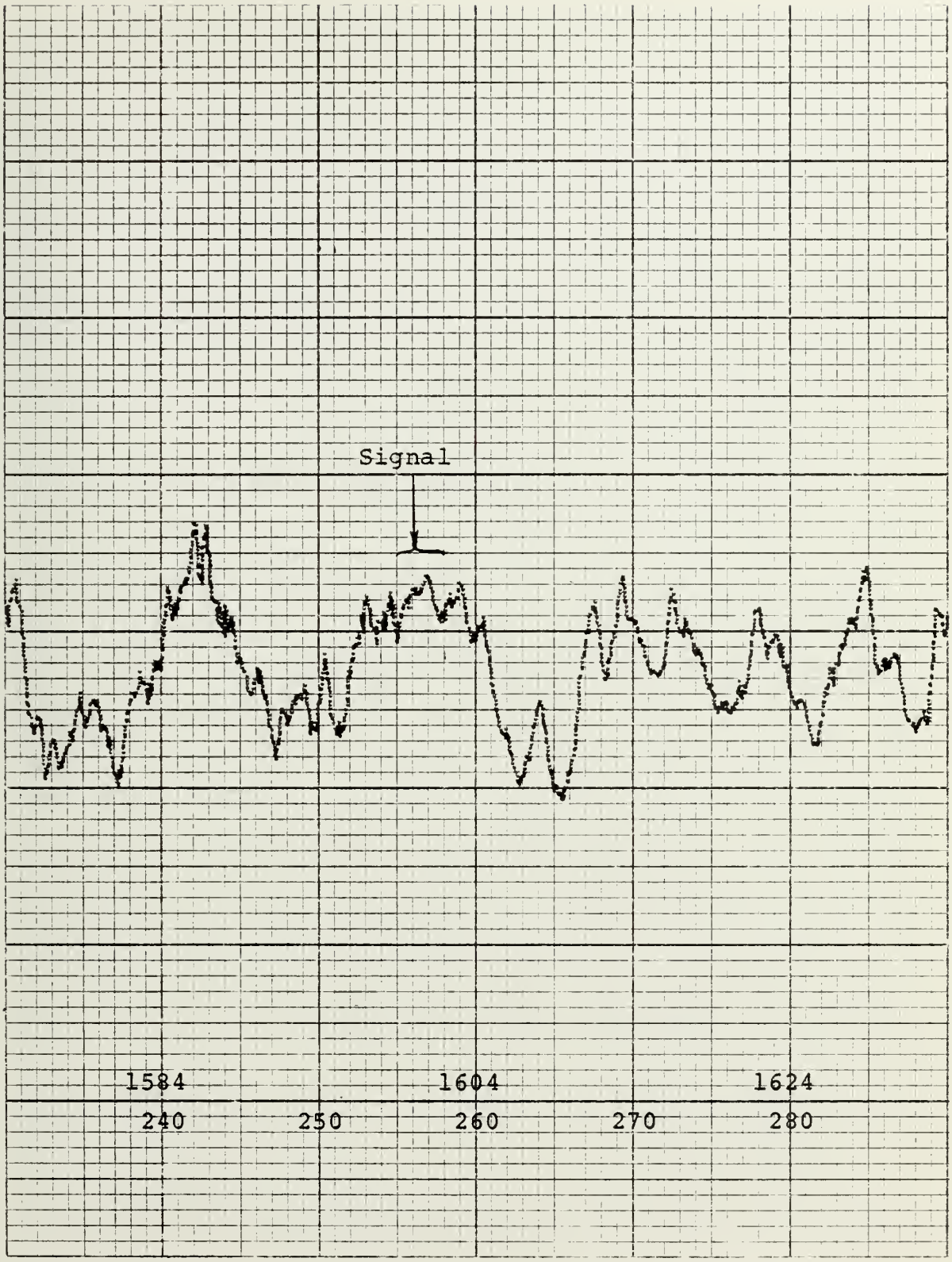

Figure 16 - SIGNAL PLUS NOISE, 6 AVE., 44 FRAMES

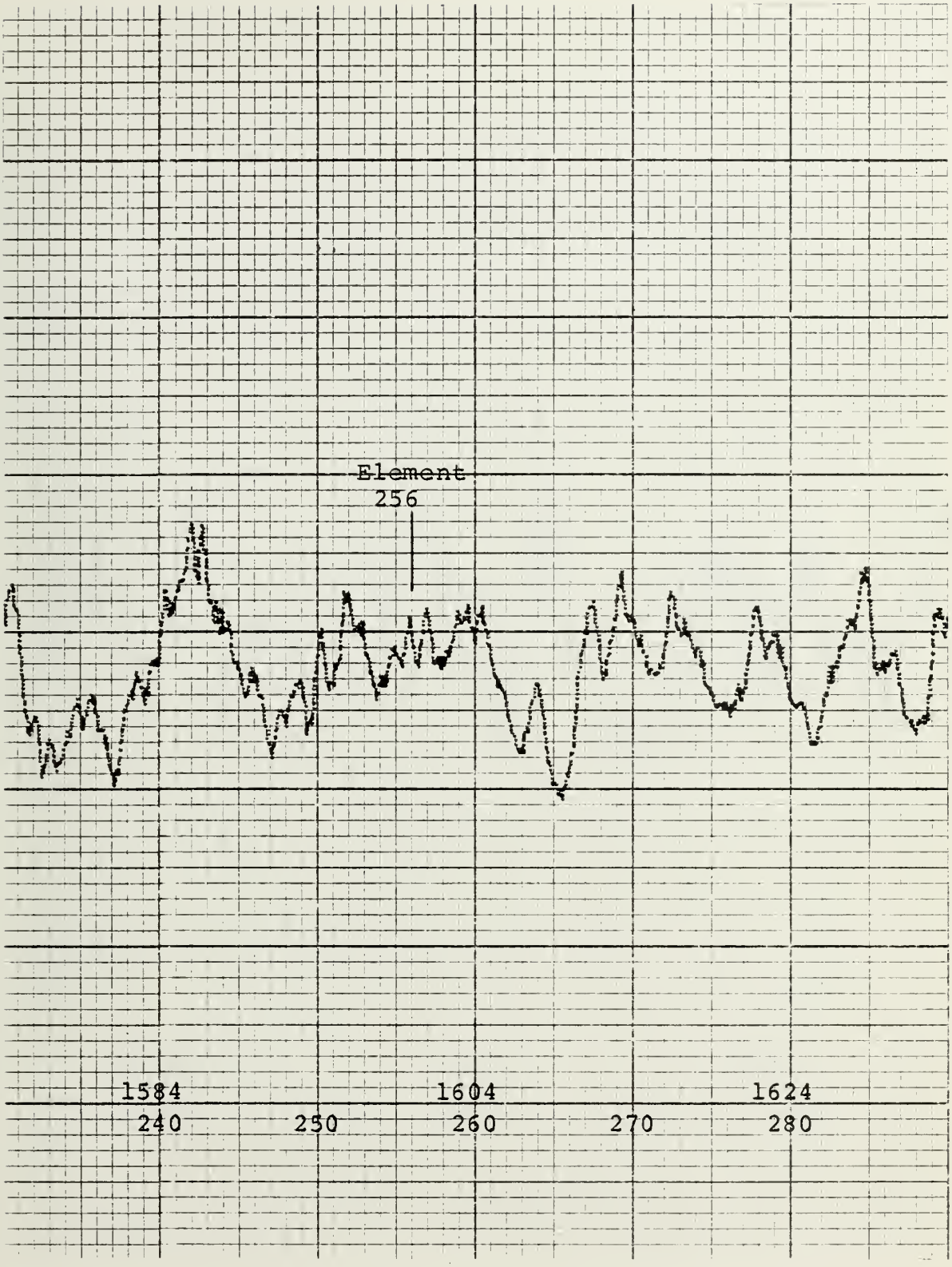

Figure 17 - NOISE, 6 AVE., 44 FRAMES

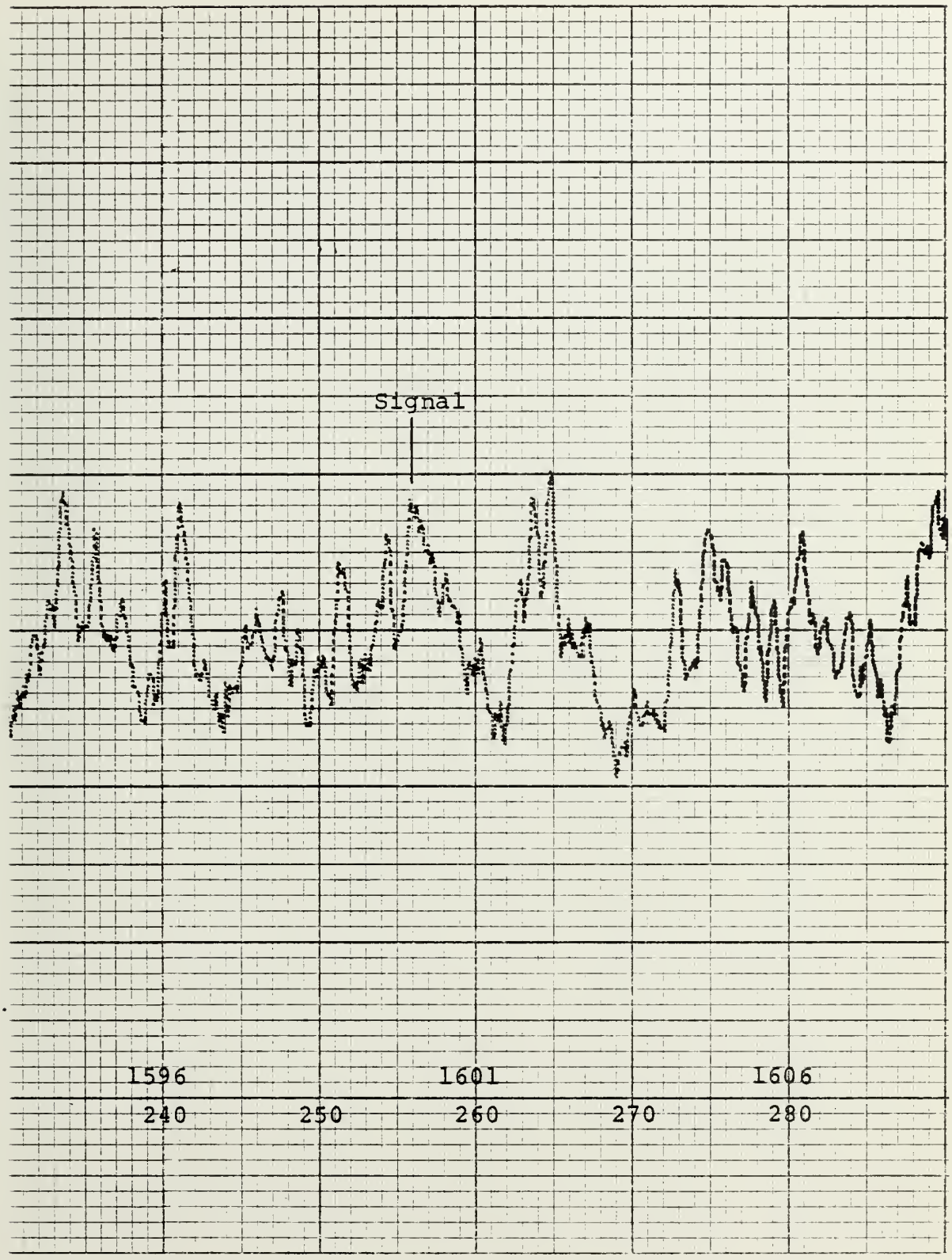

Figure 18 - RESAMPLED SIGNAL PLUS NOISE, NO AVE., 11 FRAMES

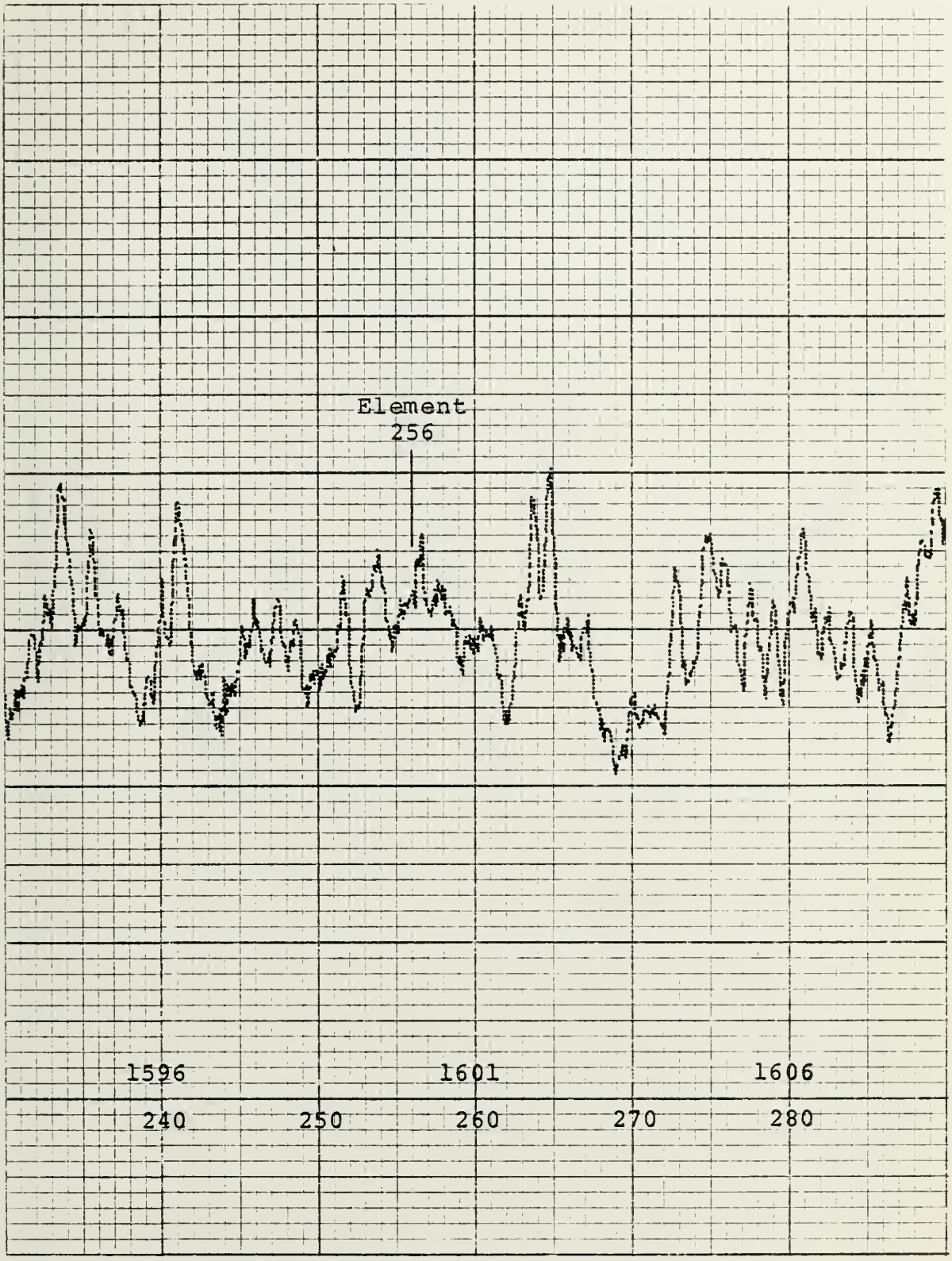

Figure 19 - RESAMPLED NOISE, NO AVE., 11 FRAMES

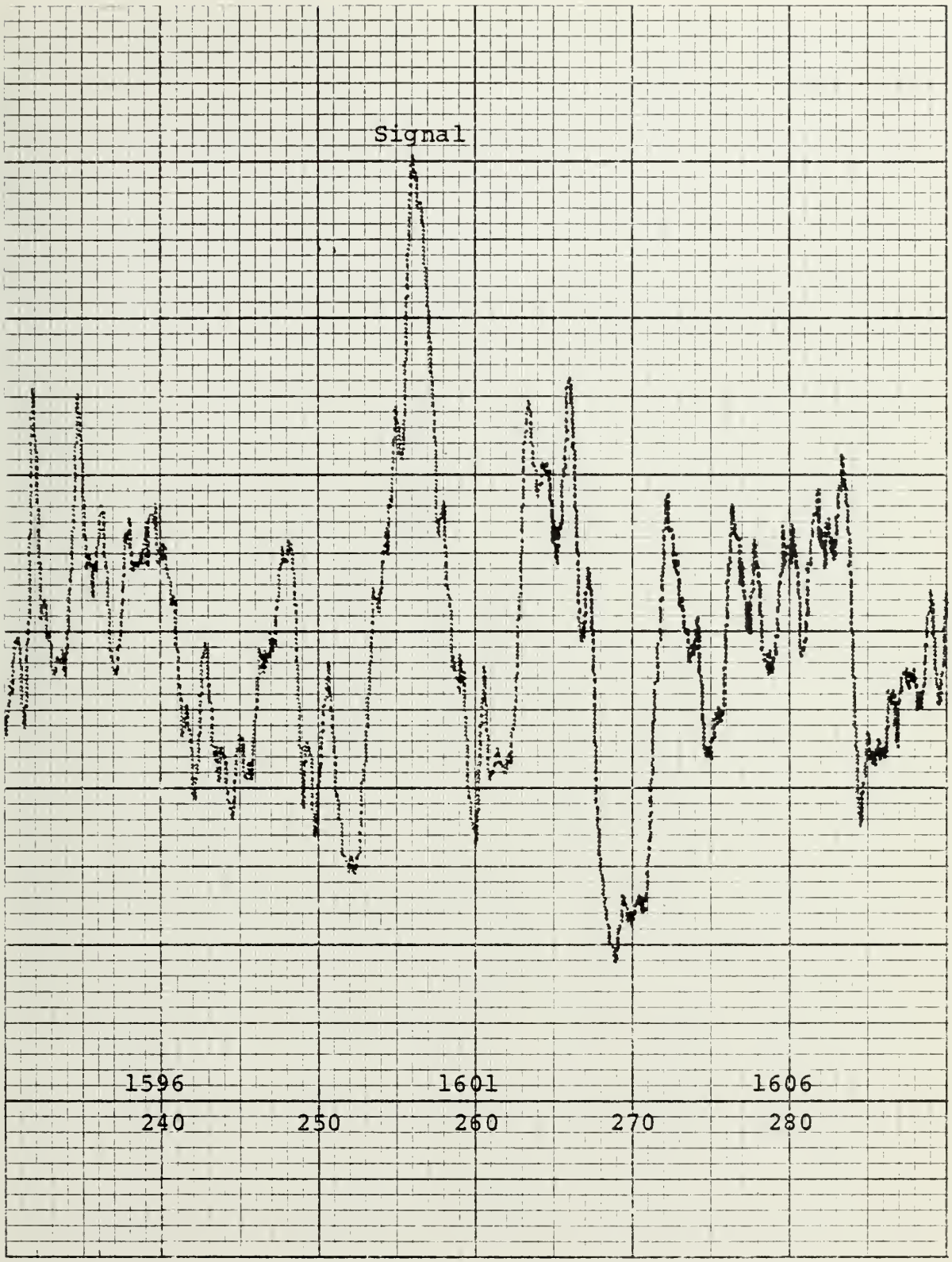

Figure 20 - rESAMPLED SIGNAL PLUS NOISE, 6 AVE ., 11 FRAMES

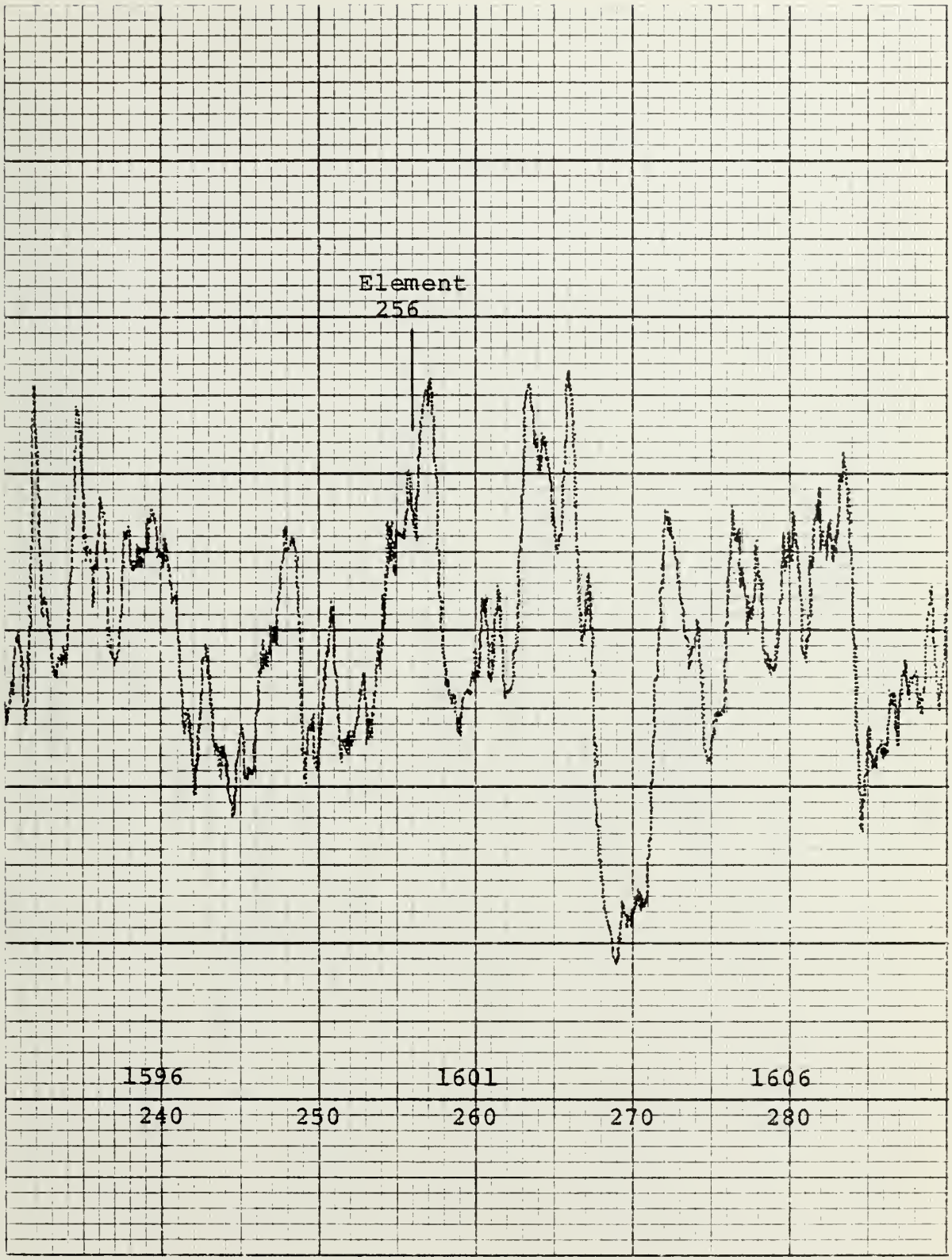

Figure 21 - RESAMPLED NOISE, 6 AVE ., 11 FRAMES

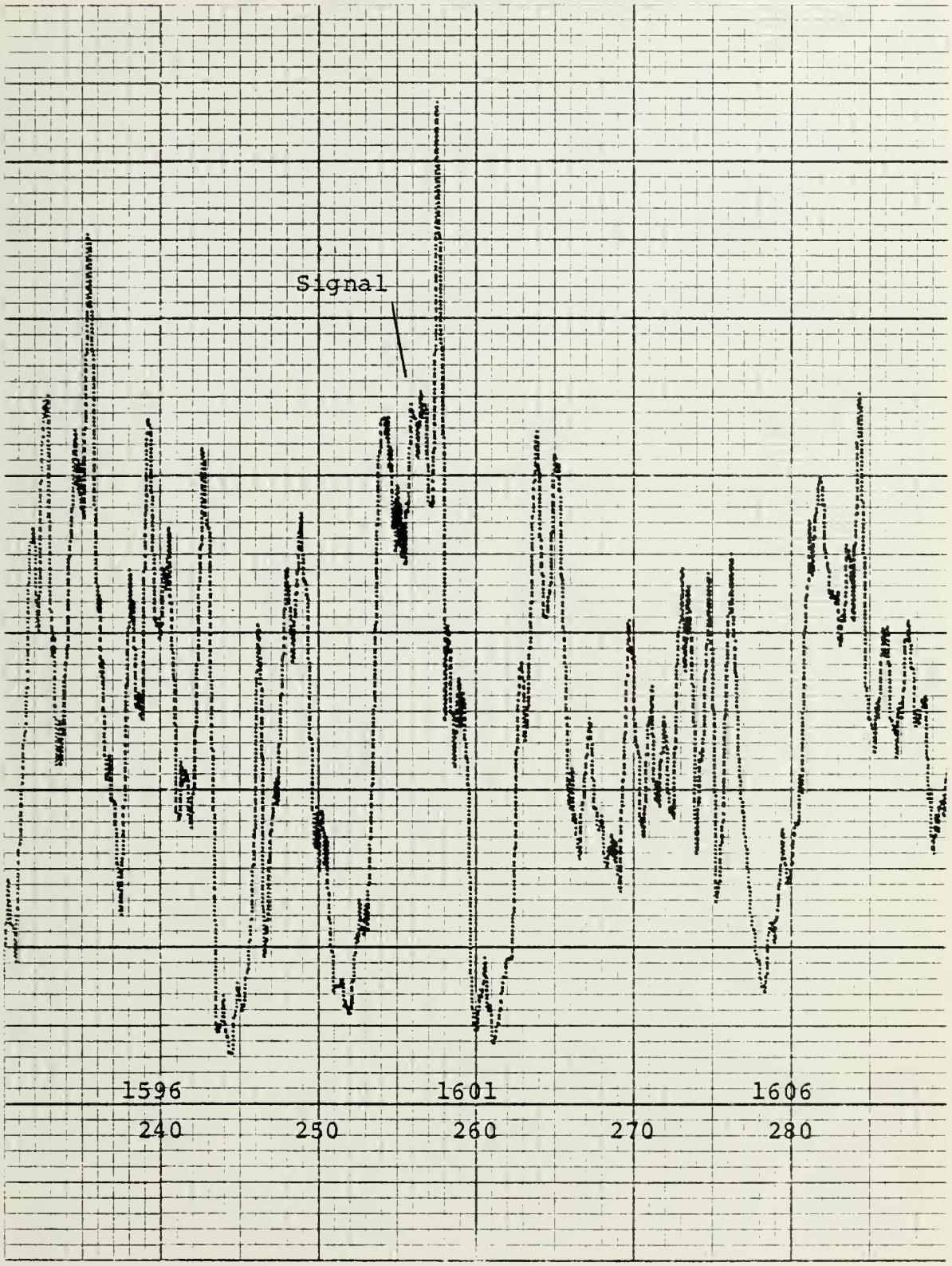

Figure 22 - RESAMPLED SIGNAL PLUS NOISE, 10 AVE., 11 FRAMES

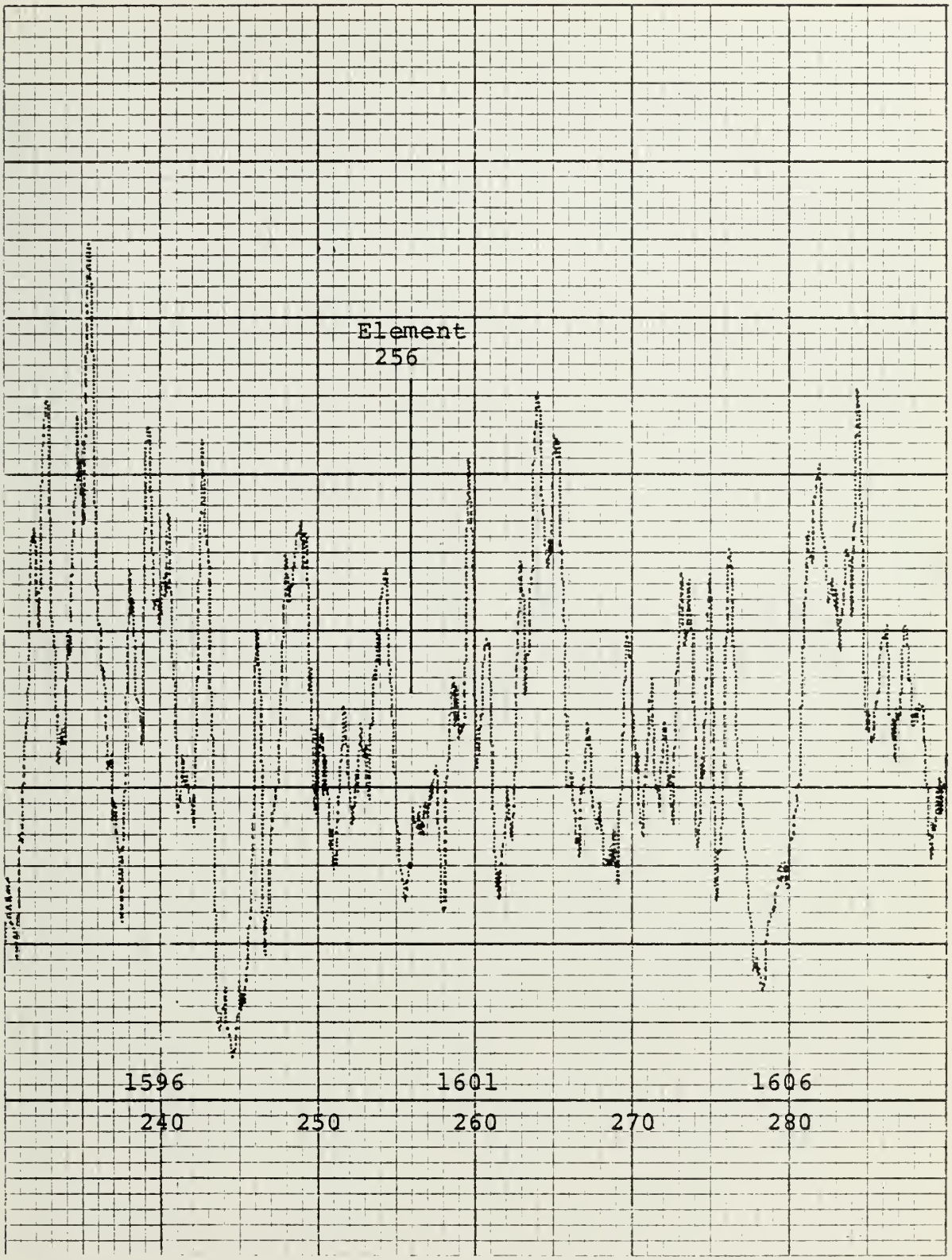

Figure 23 - RESAMPLED NOISE, 10 AVE., 11 FRAMES

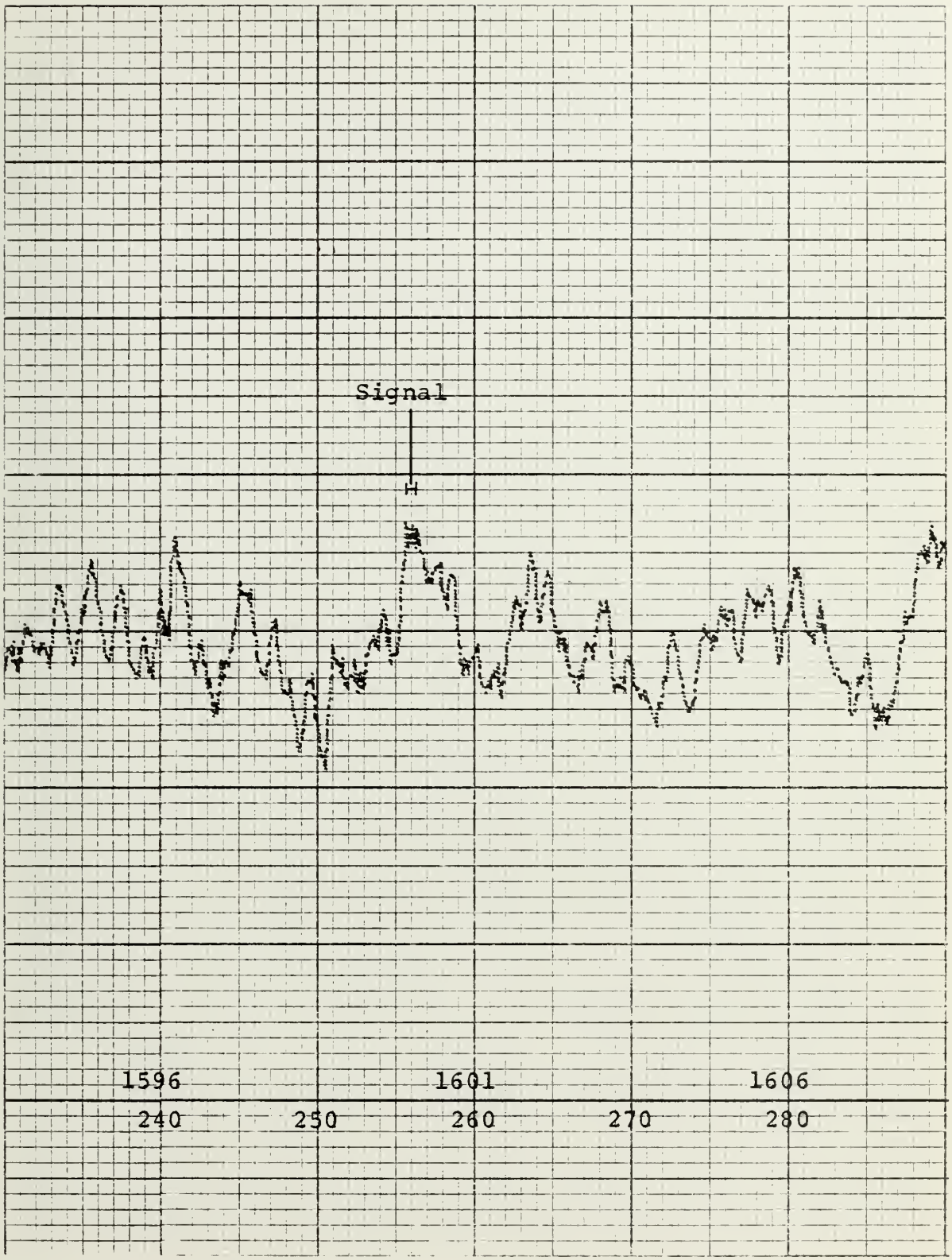

Figure 24 - RESAMPLED SIGNAL PLUS NOISE, NO AVE., 21 FRAMES

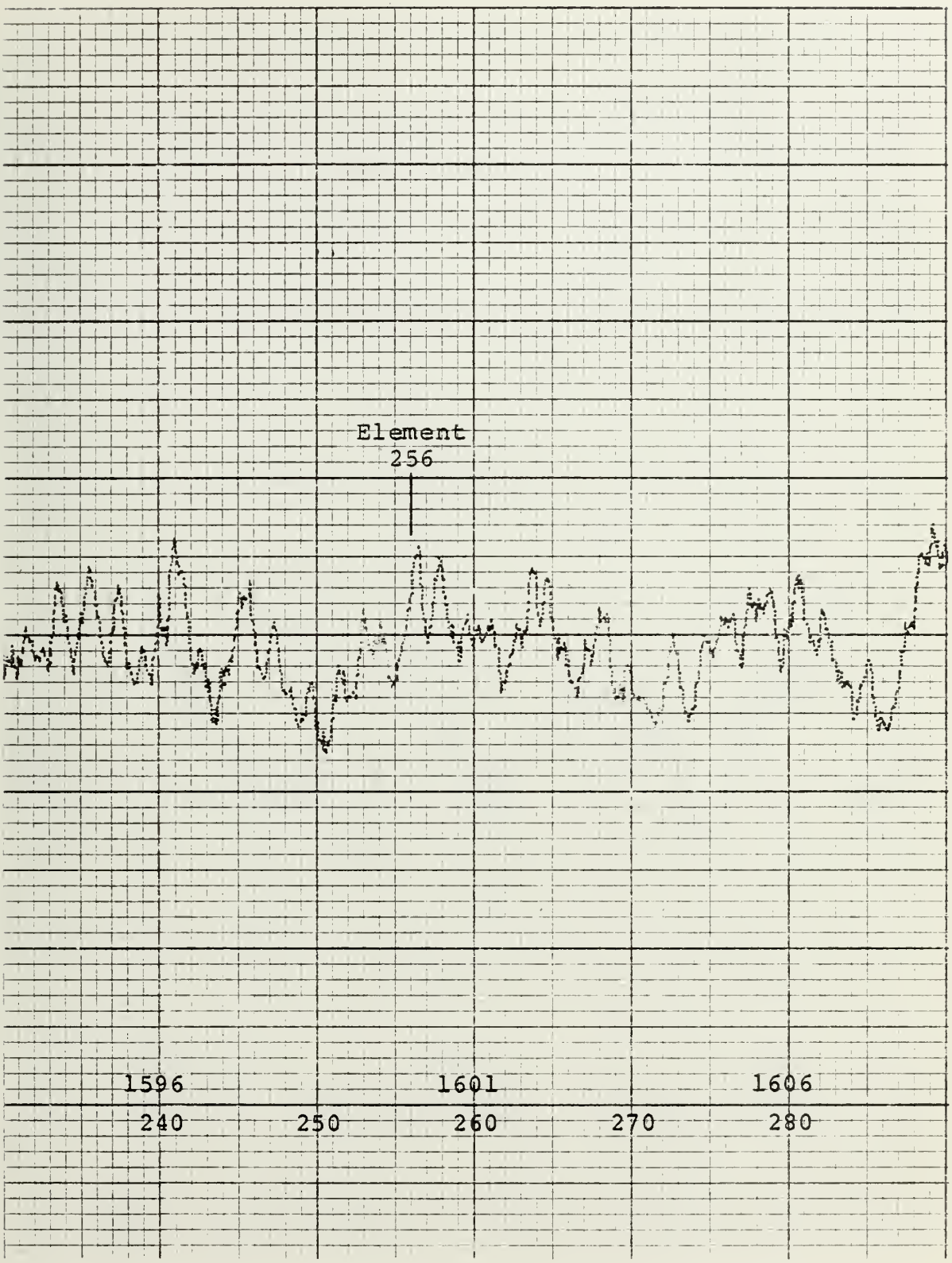

Figure 25 - RESAMPLED NOISE, NO AVERAGE, 21 FRAMES

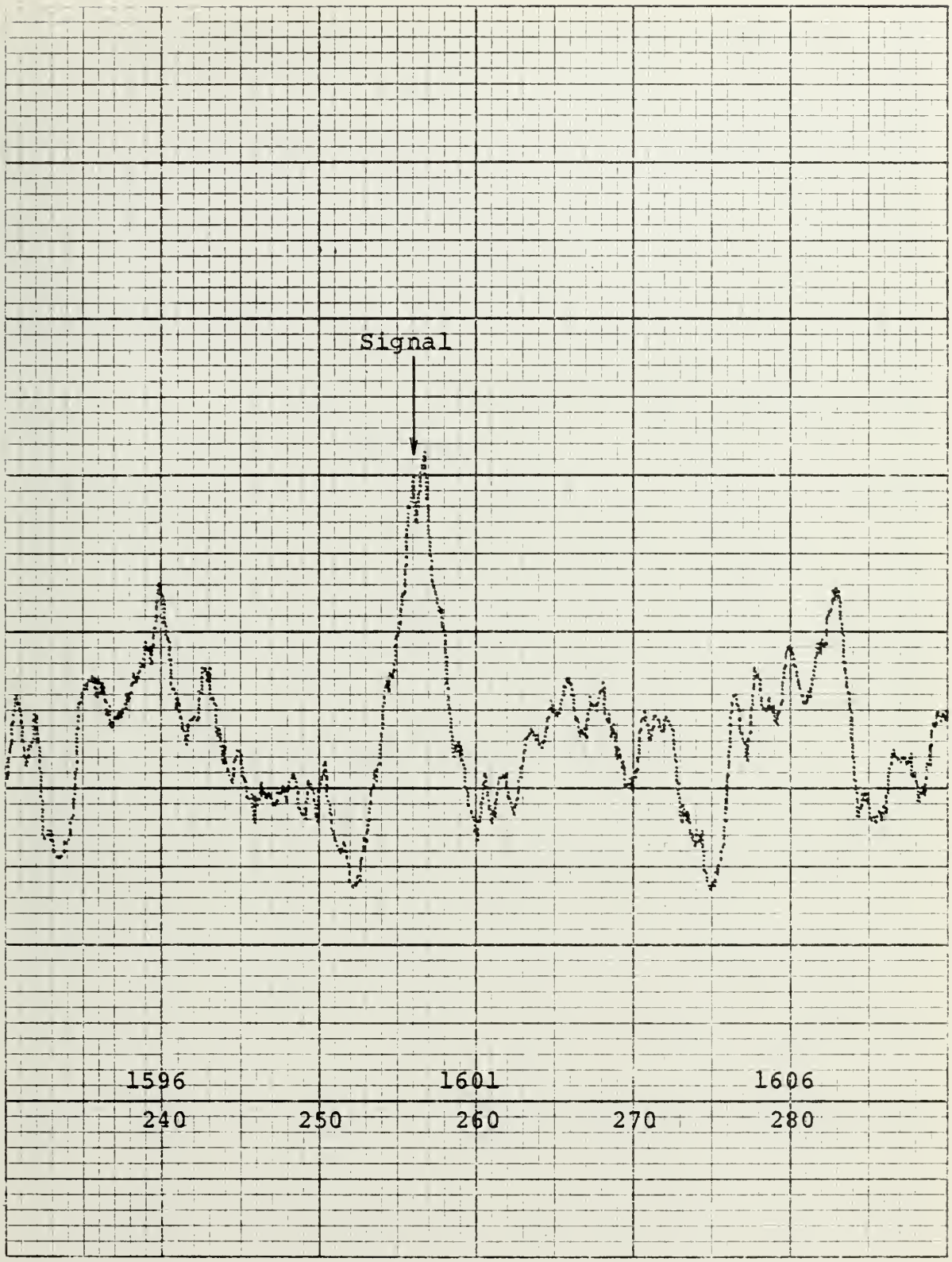

Figure 26 - RESAMPLED SIGNAL PLUS NOISE, 6 AVE., 21 FRAMES

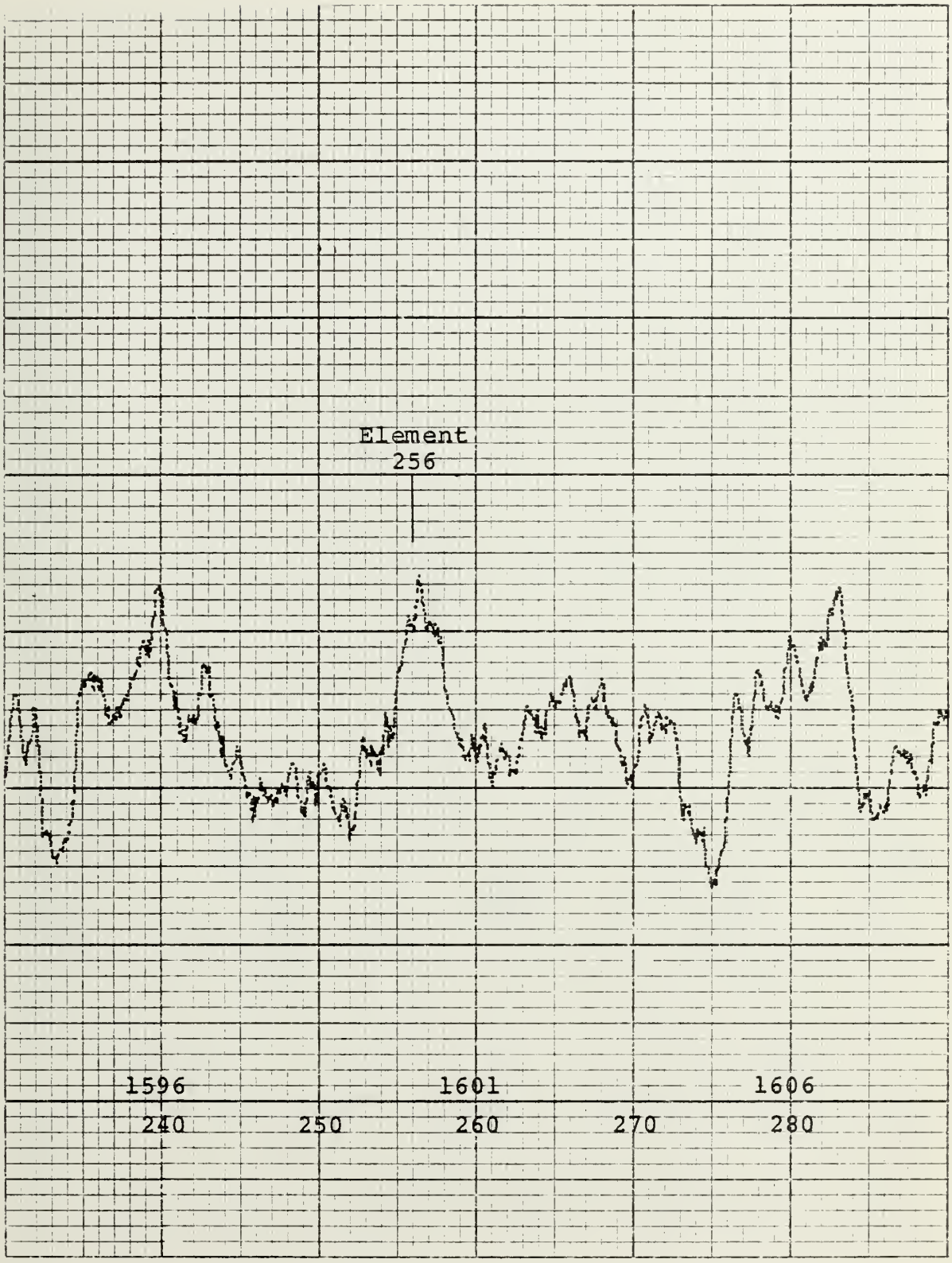

Figure 27 - RESAMPLED NOISE, 6 AVE ., 21 FRAMES

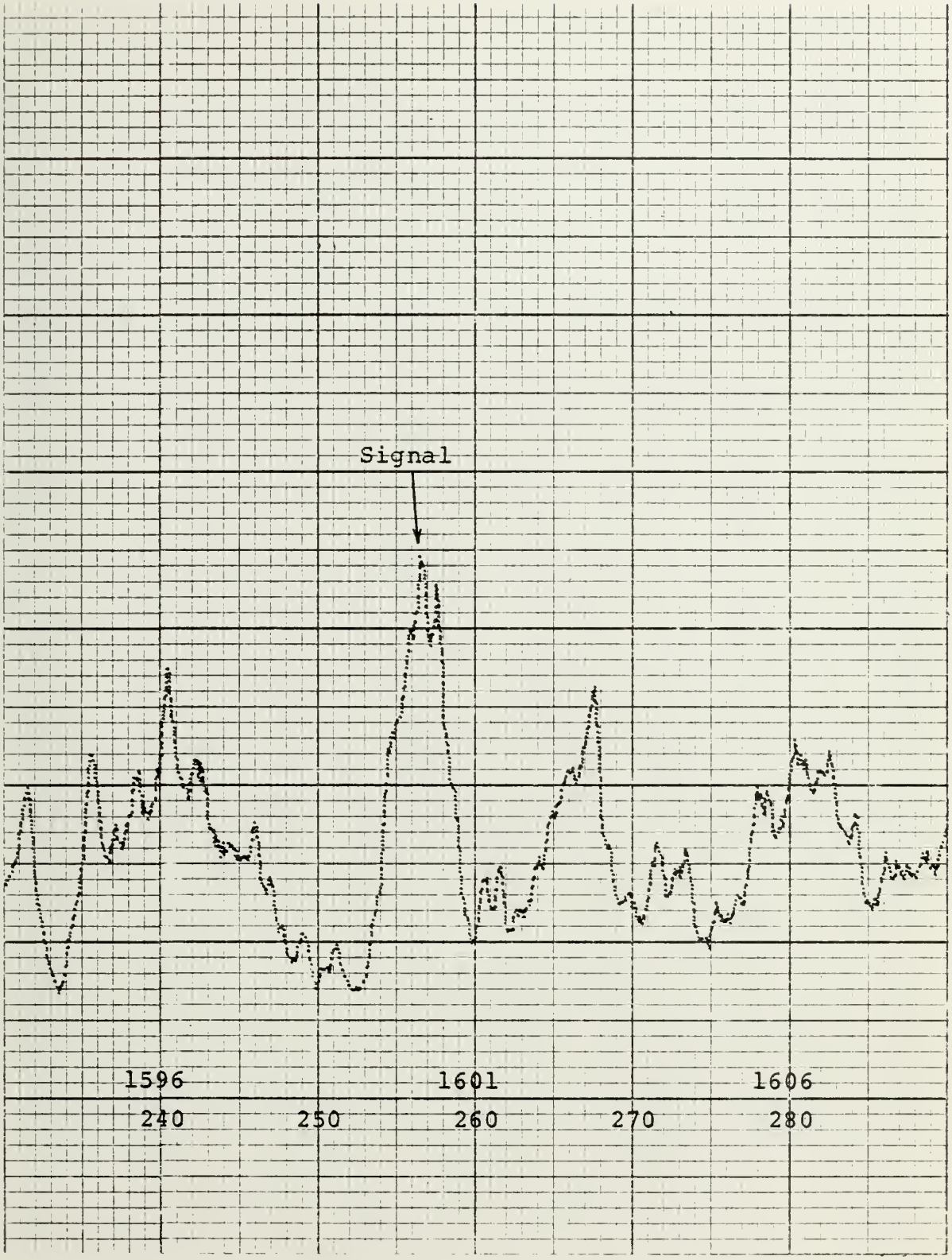

Figure 28 - RESAMPLED SIGNAL PLUS NOISE, 10 AVE., 21 FRAMES

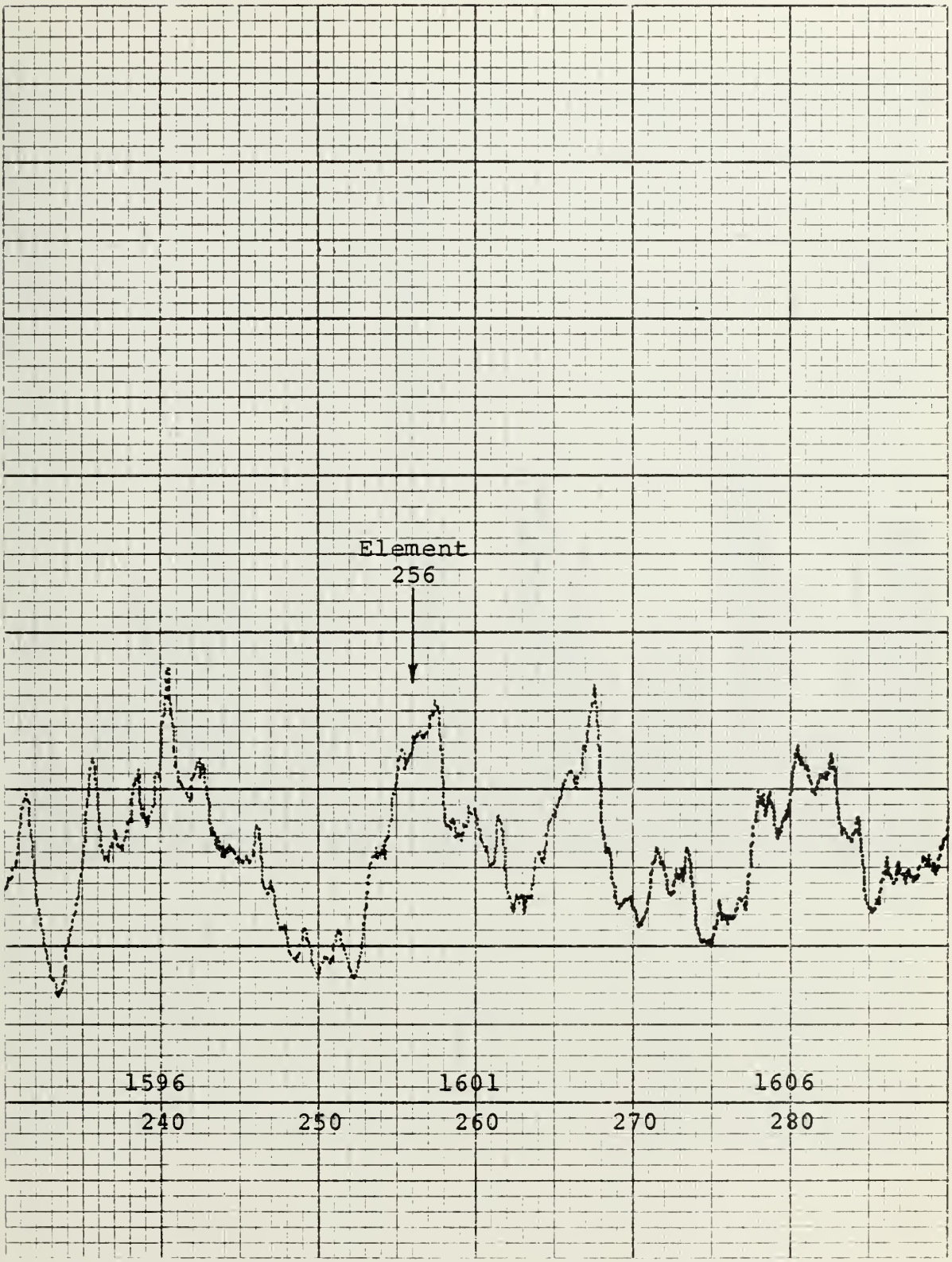

Figure 29 - RESAMPLED NOISE, 10 AVE ., 21 FRAMES

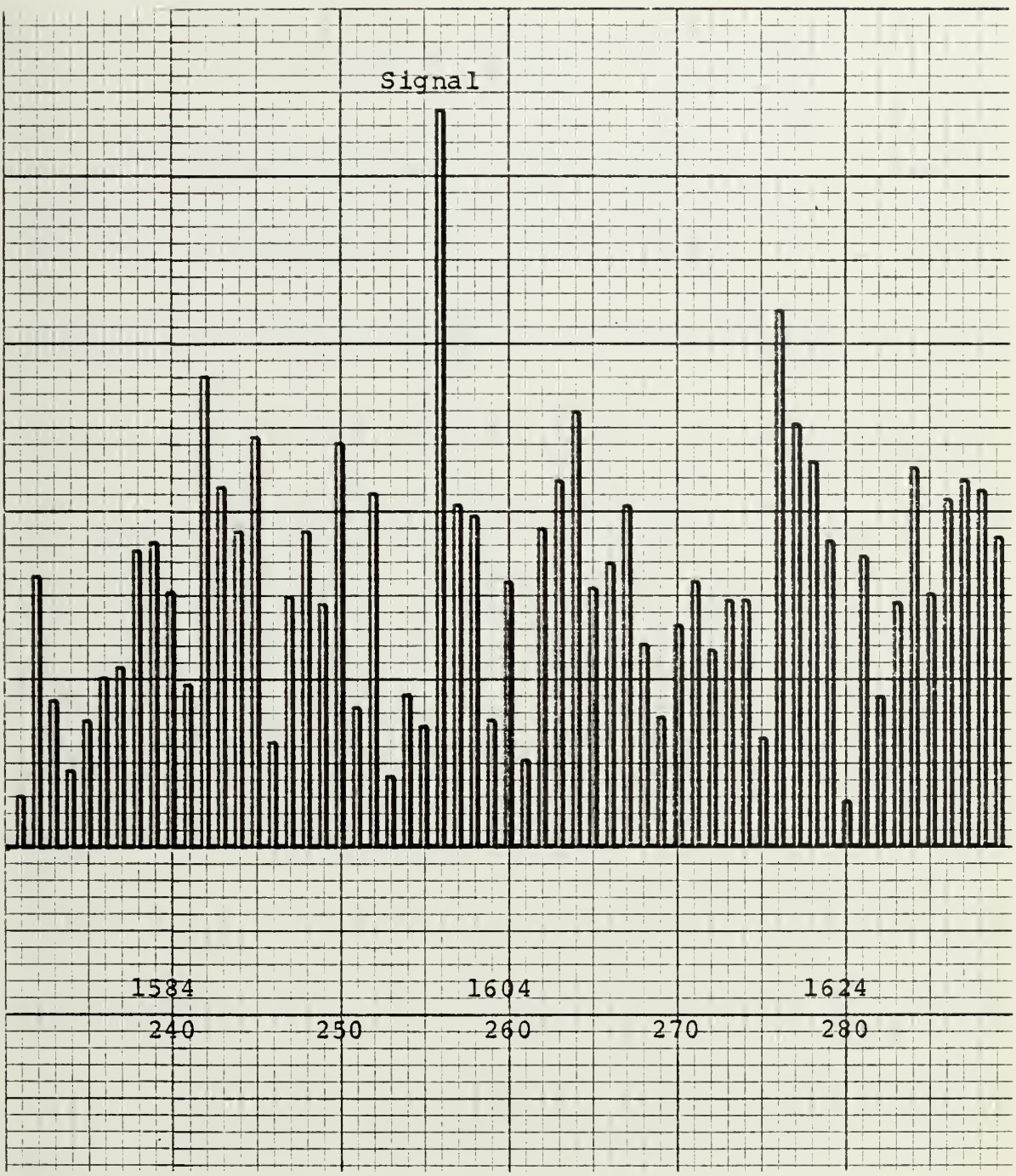

Figure 30 - AVERAGED DFT OF SIGNAL PLUS NOISE, 44 FRAMES

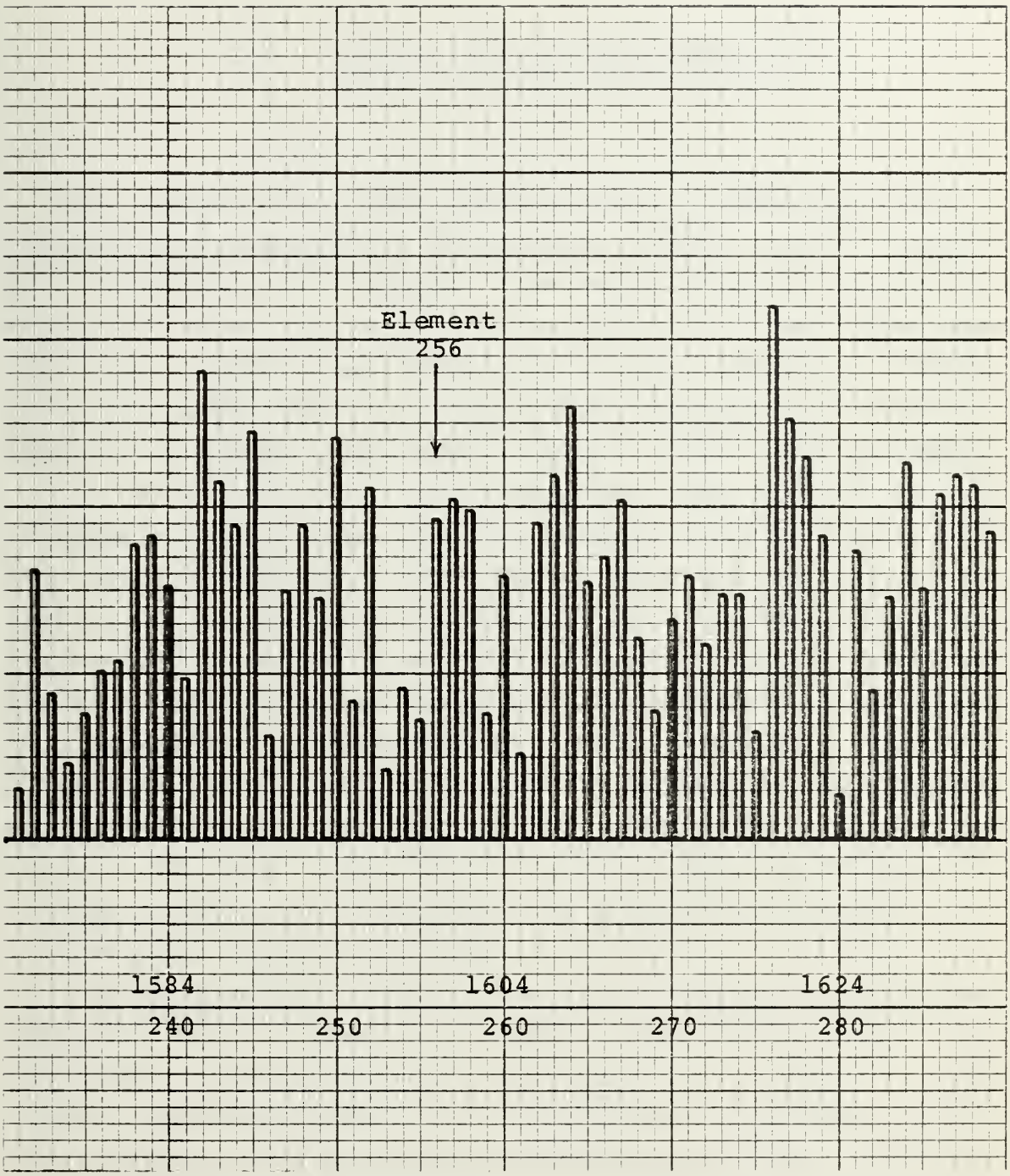

Figure 31 - AVERAGED DFT OF NOISE, 44 FRAMES

VI. CONCLUSIONS AND RECOMMENDATIONS

The purpose of this thesis was to verify the logic of tegulometric analysis in the program HISCAN and to search for techniques to improve the sensitivity of the method. After some minor program modifications, it was concluded that the method was both valid and accurate. Further investigations showed that three methods were of significant value in improving the sensitivity of HISCAN. These were:

a. DFT averaging. This technique, used in many signal processing procedures, preconditioned the data to increase the relative strength of the signal compared to the noise prior to tegulometric analysis. It is well known that lengthy DFT averages of stationary noise can improve the signal to noise ratio considerably if processing time is not an important consideration. In practice, however, processing time must be minimized to obtain results quickly and to reduce the effects of non-stationary signals and noise. It was found that 6 to 10 input DFT frames per average resulted in improvement in signal detectability for a short data acquisition time.

b. Resampling. This operation resulted in great analysis improvements by reducing the noise power per frequency element without affecting the signal power. Because HISCAN operated on a fixed number of elements in the swept filter, this resulted in a decrease in the noise power in the filter. Measurements of filtering and resampling by a factor of 4 showed a reduction in the noise power per element by a factor of about 4 as theoretically predicted. Because this method also increased the effective sample time window, the frequency resolution was improved also by a factor of 4. This benefit came, however, at the expense of

longer data acquisition times.

c. Frequency shifting. Tegulometric analysis with resampling would normally have resulted in the inability to accurately analyze about 85 percent of the frequencies within the bandwidth of the sampled data. To obviate this situation, frequency shifting was employed to move any block of DFT elements into the frequency band analyzed by HISCAN. Frequency shifting, thus, removes what would be a serious restriction.

The fundamental difference between tegulometric analysis and other methods is that this process develops a frequency probability density function. Because of this, analysis should only be long enough for the histogram to stabilize. Longer analysis periods would simply add more counts to the histogram in a stationary process or cause a blurring of the results in a non-stationary process. In the other extreme, increasing the number of DFT averages does improve detection sensitivity but at the expense of greater acquisition time. In optimizing these parameters, it was found that 6 running DFT averages over 11 frames of resampled data resulted in the unmistakable detection of a 1600 Hz tone with a signal to noise ratio of -18.5 db based on a noise bandwidth of 1 Hz. This analysis represented 44 frames of data with an acquisition time of 22 seconds. Increasing the number of DFT averages or number of HISCAN sweeps did not appreciably improve the visability of the signal.

In this investigation it was determined that tegulometric analysis methods are valid, accurate and very sensitive. Future development of this process should be directed toward the practical application of detection of signals in real noise using the methods developed in this work. In addition, research should be conducted to show the effects of non-stationary signals and noise on tegulometric analysis. Because of the method's sensitivity, it is

recommended that tegulometric analysis be developed for the passive detection and analysis of acoustical and electromagnetic signals.

LIST OF REFERENCES

1. Brigham, E. O., The Fast Fourier Transform, Prentice-Hall, 1974.

2. DELETED.

3. Dollar, S. E., Multidimensional Analysis of Electroencephalogram Using Digital Signal Processing Techniques, Naval Postgraduate School, 1973.

4. Marmont, George, Tegulometric Frequency Analysis, Naval Postgraduate School, March 1975.

5. Marmont, George, Future Development of Tegulometric Analysis, Naval Postgraduate School, August 1975.

6. Stockslager, W. E., Computer Modeling of the Electroencephalogram, Naval Postgraduate School, 1974.

INITIAL DISTRIBUTION LIST

		No. Copies
1.	Defense Documentation Center Cameron Station Alexandria, Virginia 22314	2
2.	Library, Code 0212 Naval Postgraduate School Monterey, California 93940	2
3.	Department Chairman Department Of Chemistry and Physics Naval Postgraduate School Monterey, California 93940	2
4.	Professor George Marmont Department of Electrical Engineering Naval Postgraduate School Monterey, California 93940	10
5.	Professor H. Medwin Department Of Chemistry and Physics Naval Postgraduate School Monterey, California 93940	1
6.	Captain James Wheeler, Code 03 Naval Electronics Systems Command Navy Department Washington, D.C. 20632	1
7.	LCDR K. A. Tobin (Student) Naval Sea Systems Command Navy Department Washington, D.C. 20632	1

8. Office of Naval Research 1
Attn. CAPT John C. Bajus, USN, Code 101
800 N. Quincy Street
Arlinglington, Virginia 22217

9. Commander Naval Electronics Security Engineering Center 1
Attn. Mr. Andrew Gelfend
3801 Nebraska Avenue, N.W.
Washington, D.C. 20390

10. Commander Naval Electronics Laboratory Center 1
Attn. LCDR S. E. Dollar, USN Code 1300
San Diego, California 92152

11. Director, National Security Agency 1
Attn. W-3, Dr. Jerry Cole
Fort George G. Meade, Maryland 20755